AN EFFECTIVENESS EVALUATION METHOD FOR AIRBURST PROJECTILES

A THESIS SUBMITTED TO
THE GRADUATE SCHOOL OF NATURAL AND APPLIED SCIENCES
OF
MIDDLE EAST TECHNICAL UNIVERSITY

BY

OKTAY SAYGIN

IN PARTIAL FULLFILLMENT OF THE REQUIREMENTS
FOR
THE DEGREE OF MASTER OF SCIENCE
IN
ELECTRICAL AND ELECTRONICS ENGINEERING

MAY 2011

Approval of the thesis:

AN EFFECTIVENESS EVALUATION METHOD FOR AIRBURST PROJECTILES

submitted by **OKTAY SAYGIN** in partial fulfillment of the requirements for the degree of **Master of Science in Electrical and Electronics Engineering Department, Middle East Technical University** by,

Prof. Dr. Canan Özgen
Dean, Graduate School of **Natural and Applied Sciences** _____

Prof. Dr. İsmet Erkmen
Head of Department, **Electrical and Electronics Engineering** _____

Prof. Dr. Erol Kocaoğlan
Supervisor, **Electrical and Electronics Engineering Dept., METU** _____

Examining Committee Members:

Prof. Dr. Mübeccel Demirekler
Electrical and Electronics Engineering Dept., METU _____

Prof. Dr. Erol Kocaoğlan
Electrical and Electronics Engineering Dept., METU _____

Prof. Dr. Kemal Leblebicioğlu
Electrical and Electronics Engineering Dept., METU _____

Asst. Prof. Dr. Afşar Saranlı
Electrical and Electronics Engineering Dept., METU _____

Dr. Hüseyin Yavuz
ASELSAN Inc. _____

Date: _____

I hereby declare that all information in this document has been obtained and presented in accordance with academic rules and ethical conduct. I also declare that, as required by these rules and conduct, I have fully cited and referenced all material and results that are not original to this work.

Name, Last name : Oktay SAYGIN

Signature :

ABSTRACT

AN EFFECTIVENESS EVALUATION METHOD
FOR AIRBURST PROJECTILES

Saygın, Oktay

M. S., Department of Electrical and Electronics Engineering
Supervisor: Prof. Dr. Erol Kocaoğlan

May 2011, 67 pages

Airburst projectiles increase the effectiveness of air defense, by forming clouds of small pellets. In this work, in order to evaluate the effectiveness of airburst projectiles, Single Shot Kill Probability (SSKP) is computed at different burst distances by using three lethality functions defined from different measures of effectiveness. These different measures are target coverage, number of sub-projectile hits on the target and kinetic energy of sub-projectiles after burst. Computations are carried out for two different sub-projectile distribution patterns, namely circular and ring patterns. In this work, for the determination of miss distance, a Monte Carlo simulation is implemented, which uses Modified Point Mass Model (MPMM) trajectory equations. According to the results obtained two different distribution patterns are compared in terms of effectiveness and optimum burst distance of each distribution pattern is determined at different ranges.

Keywords: Airburst Projectile, Burst Distance, Target Coverage, Single Shot Kill Probability (SSKP)

ÖZ

HAVADA PARALANAN MÜHİMMATLAR İÇİN
BİR ETKİNLİK DEĞERLENDİRME METODU

Saygın, Oktay

Yüksek Lisans, Elektrik Elektronik Mühendisliği Bölümü
Tez Yöneticisi : Prof. Dr. Erol Kocaoğlan

Mayıs 2011, 67 sayfa

Havada paralanan mühimmatlar, küçük parçacık bulutları oluşturarak hava savunma etkinliğini arttırırlar. Bu çalışmada, havada paralanan mühimmatların etkinliğini değerlendirmek için, farklı etkinlik parametrelerinden tanımlanan üç hasar fonksiyonu kullanılarak, farklı paralanma mesafelerinde tek atım yok etme olasılığı hesaplanmıştır. Bu etkinlik parametreleri hedef kaplaması, hedefe vuran parçacık sayısı ve parçacıkların paralanma sonrası kinetik enerjileridir. Hesaplamalar daire ve halka şekilleri olarak adlandırılan iki farklı parçacık dağılım şekline göre gerçekleştirilmiştir. Bu çalışmada, kaçırma mesafesini belirlemek üzere Modified Point Mass Model (MPMM) yörünge denklemlerini kullanan bir Monte Carlo benzetimi uygulanmıştır. Elde edilen sonuçlara göre iki farklı dağılım şekli etkinlik açısından karşılaştırılmış ve her bir dağılım şekli için farklı menzillerde en iyi paralanma mesafesi belirlenmiştir.

Anahtar Kelimeler: Havada Paralanan Mühimmat, Paralanma Mesafesi, Hedef Kaplaması, Tek Atım Yok Etme Olasılığı

To My Love

ACKNOWLEDGEMENTS

I would like to express my sincere thanks and gratitude to my supervisor Prof. Dr. Erol Kocaoğlan for his complete guidance, advice and criticism throughout this study.

I am grateful to my manager Dr. Hüseyin Yavuz for his participation in the committee, his valuable comments and suggestions about the thesis.

I would like to thank my colleagues in ASELSAN Inc. for their support and I would like express my special thanks to Özdemir Gümüşay and İnci Yüksel for their guidance and advice throughout my study.

I would like to thank ASELSAN Inc. for providing me a peaceful working environment and resources.

I would like to express my special appreciation to my wife for her belief and encouragements.

TABLE OF CONTENTS

LIST OF FIGURES

FIGURES

LIST OF TABLES

TABLES

CHAPTER 1

INTRODUCTION

1.1 Background and Motivation

The general air defense problem is to bring a sufficiently large destructive potential at the right time to the instantaneous position of the target to be combated. The custom inputs that are taken for any fire control system are target related properties (i.e. position and velocity), projectile related properties (i.e. mass, geometry, initial velocity, initial spin rate) and environmental properties which are gravity, and atmospheric conditions.

In the simplest instance, the destructive potential for a ballistic projectile is kinetic energy. These projectiles are ineffective against fast moving and small sized targets due to errors like meteorological variations and ballistic dispersion of both weapon and projectile. In order to increase the effectiveness of air defense against these targets, it is a practical solution to utilize airburst projectiles. Airburst projectiles increase the effectiveness by forming clouds of small pellets in front of the target trajectory.

There are many criteria for effectiveness evaluation of airburst projectiles such as burst distance and time of burst. In order to determine optimum burst distance for an airburst projectile, an optimization of a cost function is done in [1]. In that work, the variables of the objective function are target coverage, number of sub-projectile hits on the target, and hit velocity of sub-projectiles to target. The effects of several factors such as target range, target dimension, firing angle on burst distance are analyzed. The variables of the objective function in that work are also used in the scope of this work. In [2], the time of burst is optimized in order to increase the

effectiveness of time programmable airburst projectiles. The time of burst is determined according to a predetermined distance. On the other hand, in [3], a method is proposed in order to increase the effectiveness of air defense for a remotely programmable airburst projectile. After projectile is fired target is continued to be tracked during the flight of the projectile. With the better known target position, the projectile is burst accordingly, and the effectiveness of the projectile is increased.

In this work, the criteria of burst distance is used for effectiveness evaluation of airburst projectiles. Because with increasing burst distances target coverage increases but number of sub-projectile hits decreases, therefore, there should be optimum values of effectiveness and burst distances that should be found out.

1.2 Outline of The Thesis

The outline of the thesis is as follows:

In Chapter 2, the concept of airburst projectiles is explained. The descriptions of the two types of airburst projectiles, which differ according to their sub-projectile distribution, are given in this chapter.

In Chapter 3, delivery errors resulting from different sources of fire control elements are described. The expressions related to mathematical modeling of random errors and to Single Shot Kill Probability (SSKP) computation are given. The details of trajectory model utilized are explained with the related equations of motion. Then, Monte Carlo simulation implemented in order to determine miss distance is explained.

In Chapter 4, the methodology applied in order to evaluate the effectiveness of airburst projectiles is given. Three measures of effectiveness of airburst projectiles, which are target coverage, number of sub-projectile hits on the target and kinetic energy of sub-projectiles after burst, are analyzed and single shot hit and kill probabilities, are computed for two different distribution patterns. From the results of

analysis and computation, optimum burst distances are determined for each different distribution pattern.

In Chapter 5, two different distribution patterns are compared in terms of effectiveness. The thesis is concluded with the evaluations of the results obtained, and some recommendations on future work concerning effectiveness evaluation for airburst projectiles.

CHAPTER 2

AIRBURST PROJECTILES

There are multiple ways of increasing the effectiveness of barreled air defense weapon systems. One way is to fire multiple projectiles to the same target at the same time. This can be done by the same weapon system or from different weapon systems. On the contrary, the probability of hitting the target can sometimes be increased by firing the weapons in a pattern around the target, rather than directly on it. Due to errors common to all shots, it might not be the best to fire all weapons at the same time directly to the same target in a multiple projectile shot [4]. This observation leads naturally to the problem of finding the optimal pattern. However, in pattern firing there is an aim point selection and the firings does not have the same aim point in order to satisfy high damage against targets.

Besides, using airburst projectiles is another solution for increasing the effectiveness of barreled air defense weapon systems against fast and small targets. Airburst projectiles utilize sub-projectiles and form a cloud of small pellets which increases the probability of hit.

The concept of airburst projectile is based on the ejection of the sub-projectiles at a pre-calculated point, which is called “burst point”. Airburst projectiles burst at a distance d in front of the target. Fire control system determines the time of burst of the projectile to eject its sub-projectiles in front of the future target position. After burst point, the sub-projectiles move towards the target in a conical or similar shape and make a sub-projectile cloud which is in tens or hundreds at the same time on the same target.

The method of activation to eject sub-projectiles is determined by the type of fuze. Using a projectile with proximity fuze may be one solution for ejection. With the signal processing taking place inside the projectile, this type of fuze bursts the

projectile and ejects its sub-projectiles in close distance to the target. Another solution is using time fuze. For this type, weapon system calculates a time of burst within very short duration and transfers this data before projectile leaves the weapon. The projectile counts down this time during its flight towards target. At the time when the zero count is reached, time fuze activates the projectile to eject its sub-projectiles. Then the sub-projectiles are directed towards the target in a conical or similar shape.

Just before burst, the projectile has a linear velocity in its longitudinal direction, and an angular velocity around its direction of motion, due to its spinning. With the linear and radial velocity components, sub-projectiles move towards the target in a conical envelope. The magnitudes of velocity components determine the angle of this conical volume. If the magnitude of radial velocity increases relative to linear velocity, burst angle α increases. (Figure 2.1)

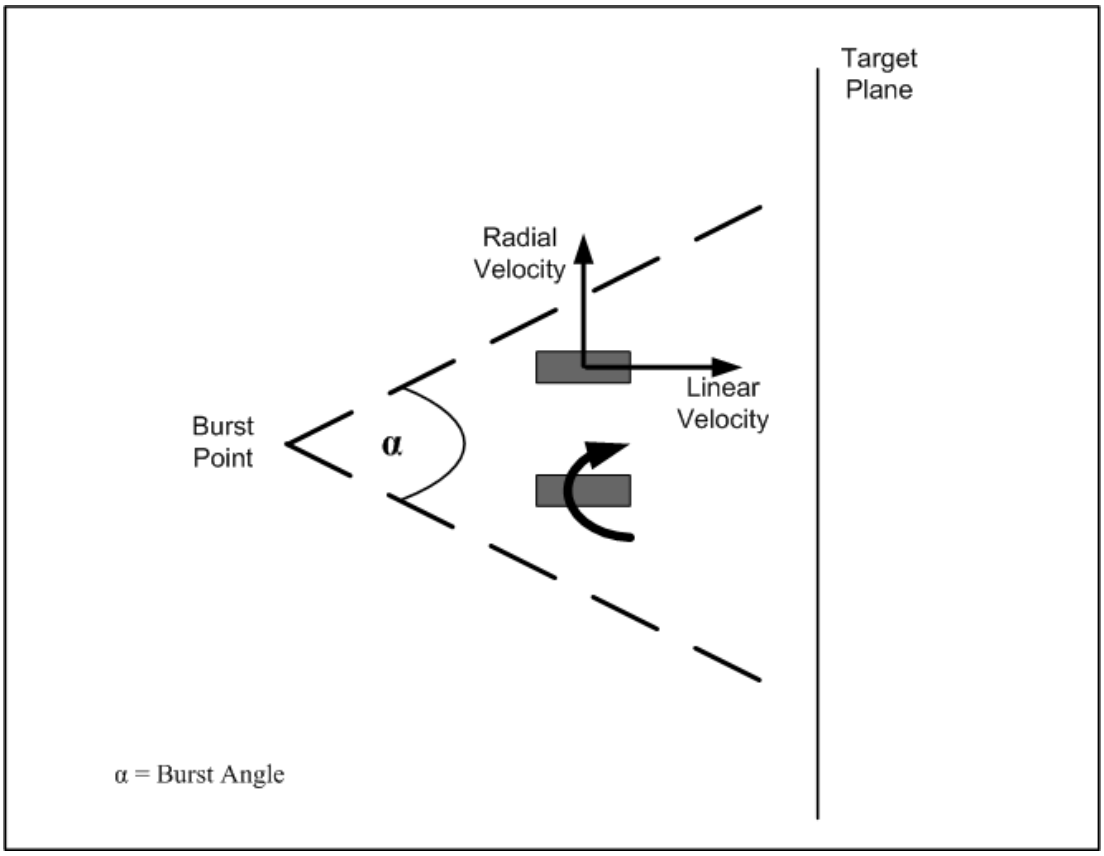

Figure 2.1: Burst angle representation

Time of burst of an airburst projectile is flight time of the projectile to the ideal impact point less a lead time, which should be determined optimally on the basis of the conditions at the time. The lead time determines the distance *d* between burst point and instantaneous target position.

In order to cover the uncertainties of both the projectile position, and target positions, this distance should be high. However, in order to deliver a sufficient kinetic energy on the target area this distance should be small which results in higher number of sub-projectiles hit on the target and high penetration capabilities. Therefore, for the effectiveness evaluation of airburst projectiles, there are many criteria that should be considered. These criteria are as follows:

- Number of sub-projectiles inside a single projectile
- Mass of each sub-projectile
- Geometry and installation of sub-projectiles (form-fit factor)
- Burst angle of projectile
- Burst distance of projectile from the target

Increasing the number of sub-projectiles inside a single projectile is going to increase the effectiveness. Since a projectile has "limited" dimensions and geometry, increasing the number of sub-projectiles decreases the mass of each sub-projectile. Therefore, there is a trade-off in terms of effectiveness between the number of projectiles and the mass of each sub-projectile.

Another criterion is burst angle of projectile and this is related to the spin rate and the linear velocity of the projectile. With a high burst angle, sub-projectiles can cover a large area on the target but since the sub-projectiles are scattered in a large volume, number of sub-projectiles per unit area decreases. On the contrary, with a low burst angle the number of sub-projectiles per unit area increases but for this time the coverage area of target decreases. There is again a trade-off in terms coverage and number of sub-projectile hits on the target. Same situation is valid for burst distance of projectile from the target. Increasing the distance of burst point from the target, increases the coverage but decreasing this distance decreases the number of sub-

projectile hits on the target. As a result, there should be optimum values of effectiveness and burst distances that should have to be found out for airburst projectiles.

Therefore, the geometry of the projectile, number of sub-projectiles inside the projectile, mass of each sub-projectile and the installation of sub-projectiles inside the projectile should have to be optimally determined in order to have the best burst angle for an effective airburst projectile.

In this work, for effectiveness evaluation of airburst projectiles, objective is to evaluate the effectiveness of airburst projectiles at different burst distances;

- For different types of airburst projectiles
- At different target ranges
- For a representative rectangular target

Different measures of effectiveness for airburst projectiles, such as target coverage and number of sub-projectile hits are analyzed and Single-Shot Kill Probability (SSKP) is computed at different burst distances. From the computation results, optimum burst distances are determined for two different distribution patterns.

2.1 Different Distribution Patterns

In what pattern sub-projectiles move and hit on the target, is dependent on many factors. These factors are:

- placement of sub-projectiles in the projectile
- geometry of each sub-projectile
- means of releasing the sub-projectiles
- magnitudes of the initial velocity components of sub-projectiles
- environmental conditions

Airburst projectiles may differ according to their sub-projectile distribution while they are moving towards the target. In this work, two different sub-projectiles distribution is determined. One is circular and the other is ring shaped patterns.

In circular shaped pattern, the sub-projectiles are assumed to be enclosed in a circular area. As time passes this circular area gets larger and the density of sub-projectiles decreases. This is because the number of sub-projectiles is constant. At the time of impact of sub-projectiles on target, the sub-projectile coverage of circular pattern over a rectangular target is illustrated in Figure 2.2.

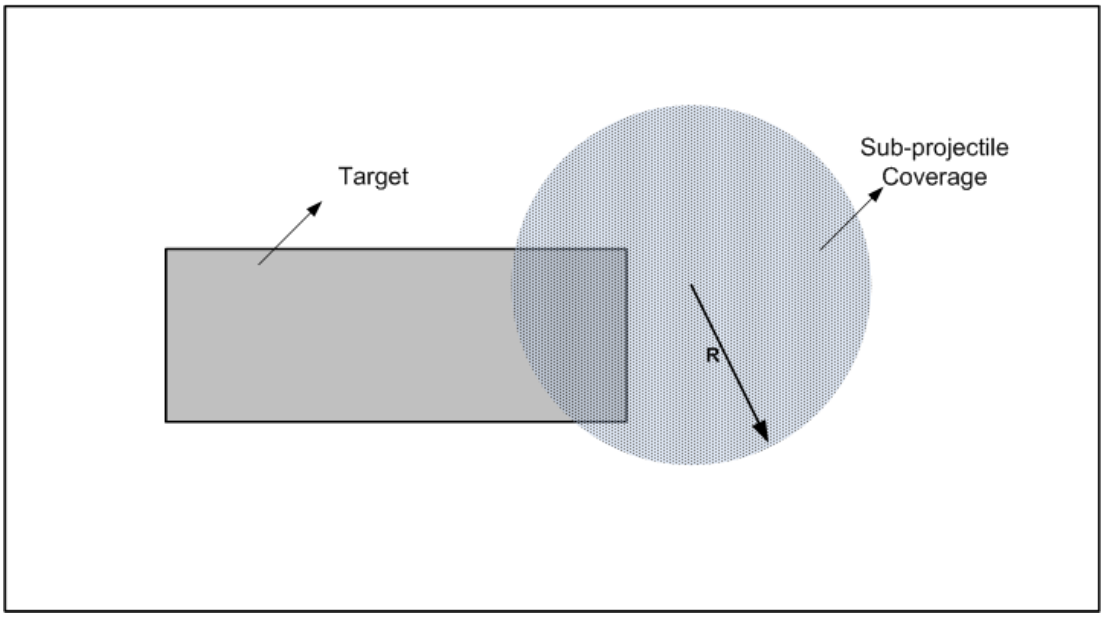

Figure 2.2: Circular distribution pattern

Another distribution pattern of sub-projectiles is ring shaped pattern. In this pattern, sub-projectiles are included in a ring shaped area. As time passes this ring gets larger and the density of sub-projectiles is decreasing since the number of sub-projectiles is fixed. Ring pattern has more sub-projectile in the unit area than circular pattern, while propagating towards target. At the time of hit of sub-projectiles on target, the sub-projectile coverage of ring pattern over a rectangular target is illustrated in Figure 2.3. r_1 is the outer radius and r_2 is the inner radius of the ring pattern.

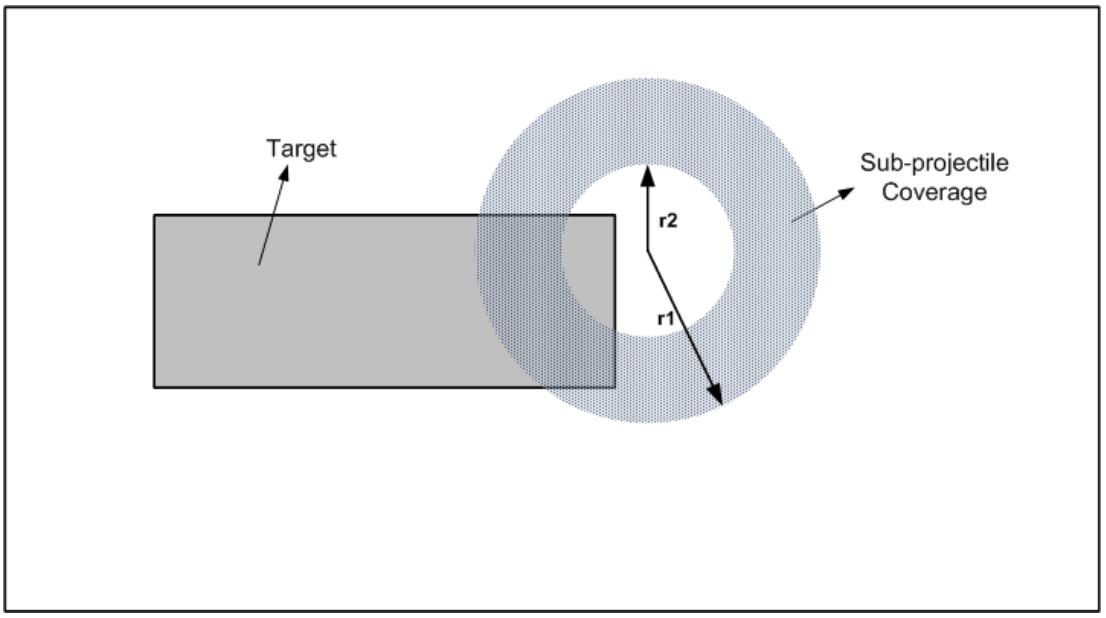

Figure 2.3: Ring distribution pattern

Airburst projectiles defeat their target with their kinetic energy. With the burst of projectile, this kinetic energy is transferred to the sub-projectiles with respect to the conservation of energy principle. Sub-projectiles carry this total kinetic energy of projectile to the target. The only difference being in the manner how they carry this potential of damage. These two different distribution patterns have different densities according to their distribution of sub-projectiles. Circular pattern carries in a lighter density than ring pattern since it has larger area of propagation [3].

CHAPTER 3

RANDOM ERRORS

Main purpose of a weapon system is to be effective against a target in order to prevent its purpose of attack. Fire control system determines azimuth and elevation orientation angles of the weapon pointing by taking into account the following inputs or data:

- Target velocity
- Weapon system velocity on which the barrels are installed
- Projectile ballistics
- Meteorological data

However, fire control systems cannot control all the errors resulting from different sources such as target position determination, weapon aiming errors, etc. There is always a difference between the predicted hit point and actual hit point and this difference is called “miss distance”. Miss distance can be separated into two components; one is in azimuth direction and the other is in elevation direction. (Figure 3.1)

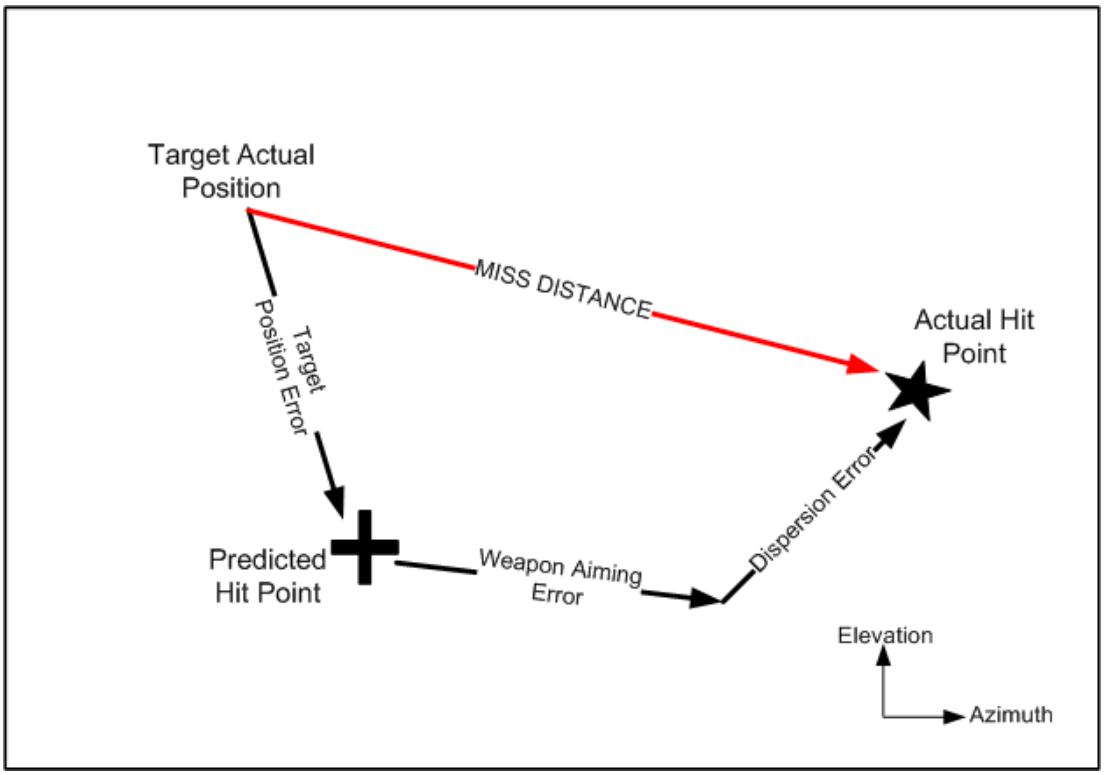

Figure 3.1: Miss distance representation

The main sources of miss distance in elevation direction due to projectile ballistics are:

- Variations in projectile mass
- Muzzle velocity variations
- Front/Tail wind
- Air density
- Air temperature

Additionally, the main sources of miss distance in azimuth direction due to projectile ballistics are:

- Muzzle velocity variations
- Lateral wind

- Gyroscopic effects resulting from the spin of the projectile

Fire control system estimates the future target position. However, since there are natural variances in the estimation algorithms and delay between measured target position and actual target position there is an error called “target position error”. Weapon pointing errors and target position errors cause delivery of projectile to a different point from actual target position. These errors are called aiming errors which are also known as bias errors [5].

3.1 Delivery Errors

Generally, delivery errors result from different sources of fire control elements. They can be decomposed into two as aiming and dispersion errors.

Aiming errors, sometimes called bias errors, are common to all firings which may be the result of gun orientation errors, target position errors, etc. On the other hand, dispersion is a measure how the projectiles differ from the Mean Point of Impact (MPI) which is the point whose coordinates are the arithmetic means of the coordinates of the separate impact points of a finite number of projectiles fired at the same aiming point under a given set of conditions. Dispersion is the result of random factors such as meteorological variations, weapon and projectile ballistic dispersion. These errors cause distribution of impact points around MPI. For a burst of five projectiles MPI, aiming error and dispersion of each projectile shot around MPI are shown in Figure 3.2.

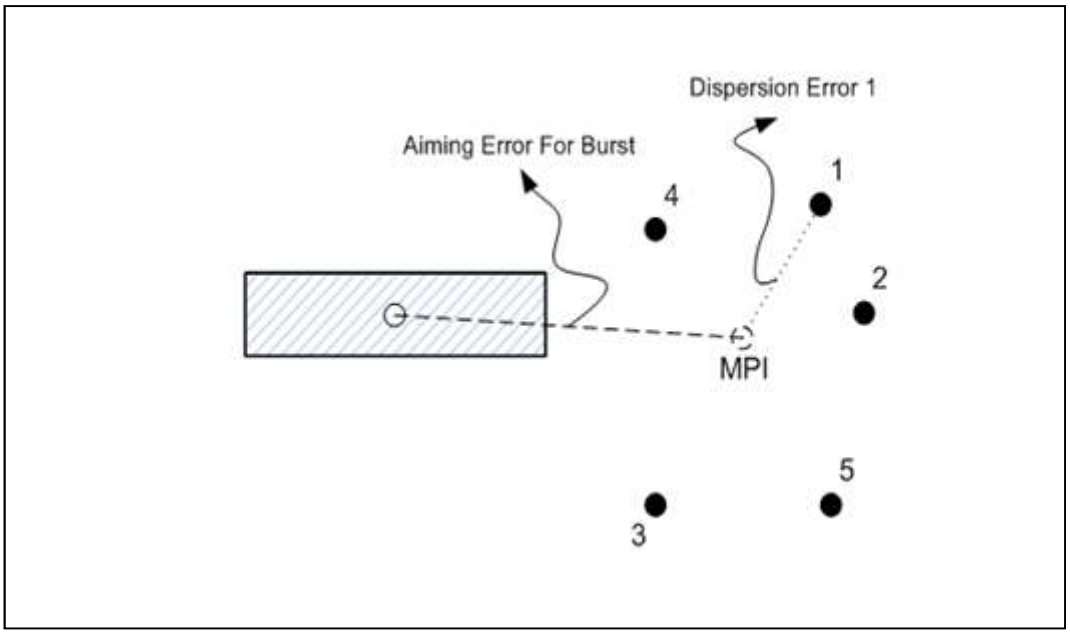

Figure 3.2: Mean Point of Impact (MPI)

Dispersion type of errors are sometimes called precision errors resulting from the muzzle velocity variations of the projectile, meteorological disturbances such as tail/front wind and the projectile dispersion properties due to manufacturing tolerances. Dispersion errors are random and they are expressed mathematically with probability density functions.

3.2 Mathematical Modeling of Random Errors

Random errors need to be accounted for in mathematical models for effectiveness considerations. Errors cause a projectile to impact at a different point from predicted hit point. Random errors are probabilistic and they can be defined with probability density functions. The custom assumption for random errors in any fire control problem is to taking them as normal probability density function. These errors occur in azimuth and elevation directions. Then, they can be assumed as bivariate normal probability density function with its variants independency. Probability density function for normal distribution is expressed with Equation (3-1).

$$p(x) = \frac{1}{\sqrt{2\pi}\sigma_x} e^{-\frac{(x-\mu_x)^2}{2\sigma_x^2}} \quad (3\text{-}1)$$

where

μ_x: The mean value of distribution in x direction

σ_x: The standard deviation value of distribution in x direction

Normal probability density function is given in Figure 3.3 with the representation of mean and standard deviation. Aiming errors and target position errors are treated as mean and the other errors are treated as standard deviation of the distribution.

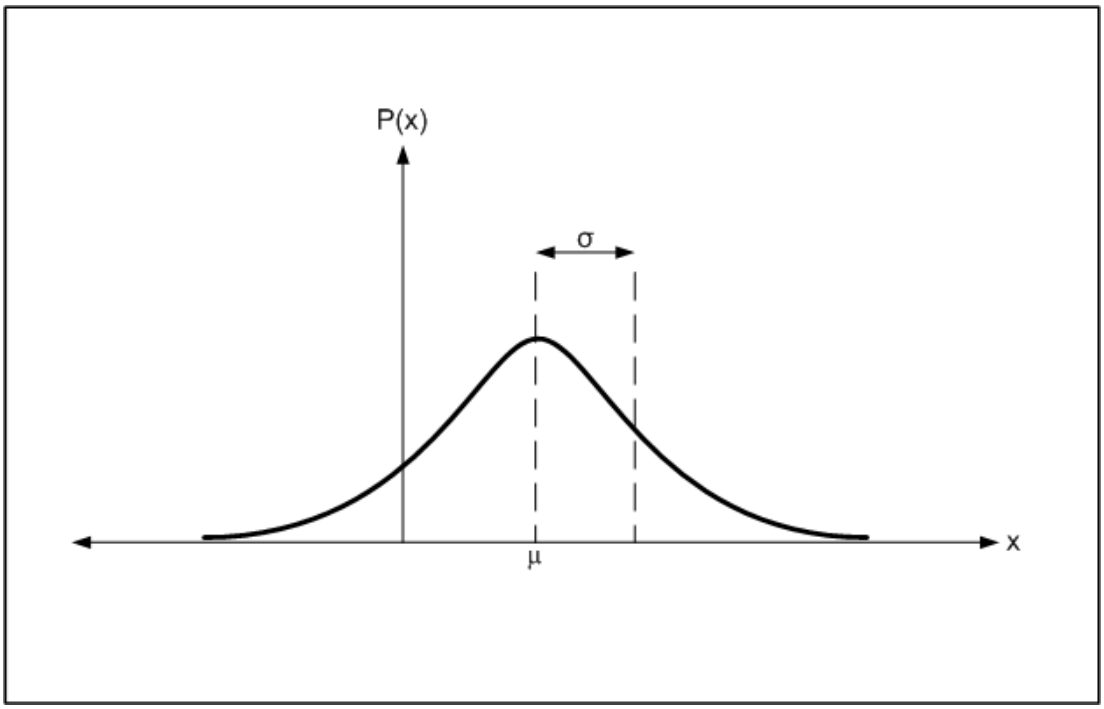

Figure 3.3: Normal probability density function

For bivariate normal distribution to characterize probability distributions of delivery errors with the assumption of independency, probability density function can be defined as the multiplication of each variants in x and y directions. (Equation (3-2))

$$p(x,y) = p(x)p(y) = \frac{1}{2\pi\sigma_x\sigma_y} e^{-\left[\frac{(x-\mu_x)^2}{2\sigma_x^2} + \frac{(y-\mu_y)^2}{2\sigma_y^2}\right]} \quad (3\text{-}2)$$

where

μ_x: The mean value of distribution in x direction

σ_x: The standard deviation value of distribution in x direction

μ_y: The mean value of distribution in y direction

σ_y: The standard deviation value of distribution in y direction

x and *y* denote the directions of the specified mean and standard deviation. The elevation direction is denoted by *y* and the azimuth direction is denoted by *x*.

To measure the effectiveness, fundamental military requirement imposed on a weapon system is the probability of kill. This measure varies according to weapon system considered since the mechanisms and projectiles used for weapon systems differ from one to another.

In this work, the general effectiveness evaluation of airburst projectiles is Single Shot Kill Probability (SSKP).

3.3 Single Shot Kill Probability

Single Shot Kill Probability (SSKP) is a performance value of damage that can be given to a target by a projectile. SSKP is defined as the product of three performance measures;

$$P_K = P_H \text{ x } P_R \text{ x } P_L \quad (3\text{-}3)$$

P_H is the probability that a projectile hits the target, P_R is the probability that the system works correctly, P_L is the probability that a specified level of damage is achieved which is usually called lethality. This measure is the conditional probability of a kill, given hit. In this work, the measure P_R (reliability) is not considered since the system reliability is out of the scope of this study and therefore; P_R is assumed to be equal to 1 for all computations.

P_H is a measure of accuracy for a weapon system. When it is assumed that the delivery errors have the characteristic behavior of bivariate normal distribution with variants independency, P_H for a shot-target combination is evaluated according to Equation (3-4). [6]

$$P_H = \frac{1}{2\pi\sigma_x\sigma_y}\int e^{-\left[\frac{(x-\mu_x)^2}{2\sigma_x^2}+\frac{(y-\mu_y)^2}{2\sigma_y^2}\right]}dA \tag{3-4}$$

where

A: The target area of integration

P_L is lethality measure and it is represented by lethality functions. Let $l(x,y)$ be a lethality function or damage function denoting the probability of target destruction when the projectile impact point is at (x,y) where x is the distance in azimuth, y is the distance in elevation relative to predicted aim point. Then, $l(x,y)$ represents the likelihood of target destruction when impact point is (x,y).

When actual impact point of a single projectile is at (x,y) and denoted lethality function is expressed as $l(x,y)$ then Single-Shot Kill Probability (SSKP) can be expressed by Equation (3-5), where the expression for $p(x,y)$ is given by Equation (3-2).

$$P_K = \int_{-\infty}^{\infty}\int_{-\infty}^{\infty} l(x,y)p(x,y)dxdy \tag{3-5}$$

In order to evaluate the effectiveness of an air defense weapon system, basic measures are hit and kill probabilities. Hit probability measures success on the likelihood of scoring just a hit on the target but kill probability is a comprehensive measure and dependent on many factors: [7]

- Detailed knowledge of position of impact on target
- Size, mass, and impact velocity of projectile or fragment striking target
- Vulnerability characteristics of the various elements of the target

In this work, in order to evaluate the effectiveness of airburst projectiles Single Shot Kill Probability (SSKP) is computed. For SSKP computation, three lethality functions related to target coverage, number of sub-projectile hits on the target and kinetic energy of sub-projectiles after burst, are determined. However, target vulnerability characteristics are not considered in the scope of this work.

3.4 Determination of Standard Deviations of Burst Point

In order to evaluate the effectiveness of airburst projectiles, standard deviations of projectile both in azimuth and elevation directions should be determined. In this work, a Monte Carlo simulation is implemented which determines the effects of three distinct random errors. These errors are projectile and weapon ballistics dispersion, muzzle velocity variation and wind speed variation. This simulation utilizes a comprehensive trajectory model, namely Modified Point Mass Model (MPMM). The details of the trajectory model, Monte Carlo simulation implemented and the results for standard deviations of miss distances on the target plane are given in the following sections.

3.4.1 Trajectory Model

There are simple ways of modeling the trajectory of a projectile such as zero drag, 2 Degree of Freedom (DoF) point mass models. For zero drag models only the gravity term and for 2DoF point mass models the gravity and drag terms are taken into account [8]. Moreover, there is another ballistic trajectory model which is used by NATO Armaments Ballistics Kernel (NABK) trajectory program. This program implements Modified Point Mass Model (MPMM) in order solve the fire control problem for spin stabilized projectiles. Contrary to simple ballistic trajectory models, in MPMM lift force, magnus force, and the coriolis acceleration are included in the acceleration equations, making MPMM computationally intensive [8].

In this thesis, MPMM is the fundamental trajectory model utilized to derive standard deviations of miss distance of projectile in azimuth and elevation directions. To derive an MPMM trajectory model is out of the scope of this study. The model is taken from ASELSAN resources, which is only used to determine miss distances.

The equations related to MPMM is basically derived from Newton's Second Law of Motion which gives the expression of acceleration applied to a object in terms of its mass and force applied to the object. That is, the ratio of force applied to the object and mass of the object gives the acceleration.

$$\vec{F} = m\ddot{\vec{u}} \tag{3-6}$$

where

$\vec{F}$: Net force vector applied to the object

m: Mass of the object

$\ddot{\vec{u}}$: Acceleration vector of the object

In MPMM the net force applied to a spin stabilized projectile is given according to Newton Second Law of Motion.

$$\vec{F} = m\ddot{\vec{u}} = \overrightarrow{DF} + \overrightarrow{LF} + \overrightarrow{MF} + m\vec{g} + m\vec{\Lambda} \tag{3-7}$$

where:

$\overrightarrow{DF}$: Drag force vector

$\overrightarrow{LF}$: Lift force vector

$\overrightarrow{MF}$: Magnus force vector

$m\vec{g}$: Gravitational force vector

$m\vec{\Lambda}$: Coriolis force vector

The evaluation of each term given above is not trivial and the expressions for each are obtained from NATO Standardization Agreement 4355 (NATO-STANAG 4355) [9].

While a ballistic projectile moves in the atmosphere there is going to be an opposing force which is called air drag. Air drag is dependent on the velocity of the projectile with respect to air. Air drag mostly affects the desired range of the projectile to be achieved since it opposes the direction of the velocity vector. The acceleration due to air drag force is given according to Equation (3-8).

$$\frac{\overrightarrow{DF}}{m} = -\left[\frac{\pi\rho i d^2}{8m}\right]\left[C_{D,0} + C_{D,\alpha^2}\left(Q_D\alpha_e\right)^2 + C_{D,\alpha^4}\left(Q_D\alpha_e\right)^4\right]v\vec{v} \tag{3-8}$$

ρ: Density of air ($^{kg}/_{m^3}$)

i: Quadrant elevation fitting form factor

d: Reference diameter of projectile (m)

m: Mass of projectile (kg)

$C_{D,0}$: Zero yaw drag force coefficient

C_{D,α^2}: Quadratic drag force coefficient ($^1/_{rad^2}$)

Q_D: Yaw drag fitting factor

C_{D,α^4}: Quartic drag force coefficient ($^1/_{rad^4}$)

v: Speed of projectile ($^m/_s$)

$\vec{v}$: Velocity of projectile with respect to air ($^m/_s$)

One way for stabilizing the projectile during its flight is spinning. For a projectile spinning in the clockwise direction, an upward force during its flight causes the nose of the projectile yawing to the right. The angle of this yaw is known as the "Yaw of Repose and is caused by the gyroscopic reaction of the projectile to the vertical angular rate as the projectile tracks the trajectory curvature causing the projectile to generate a yaw angle in the horizontal plane" [10]. The expression of yaw of repose is given by Equation (3-9).

$$\overrightarrow{\alpha_e} = \frac{8I_x p\left(\vec{v} \times \dot{\vec{u}}\right)}{\pi \rho d^3 \left(C_{M,\alpha} + C_{M,\alpha^3}\alpha_e^2\right) v^4} \tag{3-9}$$

p: Axial spin rate of projectile ($^{rad}/_s$)

I_x: Axial moment of inertia ($kg\ m^2$)

$\dot{\vec{u}}$: Acceleration of center of mass in the fixed coordinate system ($^m/_{s^2}$)

$C_{M,\alpha}$: Overturning moment coefficient

C_{M,α^3}: Cubic overturning moment coefficient ($^1/_{rad^2}$)

$$\overrightarrow{\alpha_{e_0}} = \begin{bmatrix} 0 \\ 0 \\ 0 \end{bmatrix} \tag{3-10}$$

is the initial value of yaw of repose.

The projectile moves in air during its flight. Air moves at differing velocities over the upper and lower portions of the projectile. This difference in air velocity creates a pressure differential that imparts a corresponding force to the projectile known as "dynamic lift" [11].The acceleration due to lift force is given by Equation (3-11).

$$\frac{\overrightarrow{LF}}{m} = \left[\frac{\pi \rho d^2 f_L}{8m}\right]\left[C_{L,\alpha} + C_{L,\alpha^3}\alpha_e^2 + C_{L,\alpha^5}\alpha_e^4\right]v^2\overrightarrow{\alpha_e} \tag{3-11}$$

f_L: Lift factor

$C_{L,\alpha}$: Lift force coefficient ($^1/_{rad}$)

C_{L,α^3}: Cubic lift force coefficient ($^1/_{rad^3}$)

C_{L,α^5}: Quintic lift force coefficient ($^1/_{rad^5}$)

"The Magnus effect is the physical phenomenon where the rotation of a projectile affects its trajectory when travelling through a fluid. The higher velocity above a rotating body indicated by the closer streamlines is reflected by a reduction in pressure. On the other hand, the lower velocity underneath the rotating body has a higher pressure. The net effect of these pressure changes produces a lift on the body

and an increase in range." [8] The acceleration due to magnus force is given by Equation (3-12).

$$\frac{\overrightarrow{MF}}{m} = -\frac{\pi \rho d^3 Q_M p C_{mag-f}}{8m} (\overrightarrow{\alpha_e} \times \vec{v}) \quad (3\text{-}12)$$

Q_M: Magnus factor

C_{mag-f}: Magnus force coefficient ($^1/_{rad^2}$)

The latitude of the weapon affects the range of the projectile to be reached. The rotation of the earth has an effect on the trajectory of the projectile such that it increases or decreases the range of the projectile. [11] The acceleration due to coriolis force is given according to Equation (3-13).

$$\vec{\Lambda} = -2m(\vec{w} \times \vec{u}) \quad (3\text{-}13)$$

$\vec{w}$: Velocity of the air with respect to ground ($^m/_s$)

$\vec{u}$: Velocity of projectile with respect to ground-fixed axis ($^m/_s$)

The expression for the magnitude of spin acceleration is of a projectile is given by Equation (3-14).

$$\dot{p} = \frac{\pi \rho d^4 p v C_{spin}}{8 I_x} \quad (3\text{-}14)$$

C_{spin}: Spin damping moment coefficient

The magnitude of spin is given by Equation (3-15) at time equals to t where p_0 is the initial spin rate of projectile.

$$p = p_0 + \int_0^t \dot{p}dt \tag{3-15}$$

The magnitude of the initial spin of the projectile at the muzzle is given by Equation (3-16), where t_c is the twist of rifling at muzzle ($^{calibers}/_{rev}$) and u_0 is the initial speed of projectile ($^{m}/_{s}$) with respect to ground-fixed axis.

$$p_0 = \frac{2\pi u_0}{t_c d} \tag{3-16}$$

Windage jump which is the correction for wind shear between successive integration steps, is given as a velocity correction. (Equation (3-17))

$$\Delta\vec{u} = \frac{\left(C_{L,\alpha} + C_{L,\alpha^3}\alpha_e^2 + C_{L,\alpha^5}\alpha_e^4\right) f_L I_x p(\vec{u} \times \Delta\vec{w})}{\left(C_{M,\alpha} + C_{M,\alpha^3}\alpha_e^2\right) m d v^2} \tag{3-17}$$

where $\Delta\vec{w}$ is the difference in wind between integration steps given by Equation (3-18).

$$\Delta\vec{w} = \vec{w_t} - \vec{w_{t-\Delta t}} \quad (3\text{-}18)$$

and at $t = 0, \vec{w_t} = \vec{w_0} = 0$

The equations from 3-6 through 3-18 are given in order to explain the general equations of motion of a spin stabilized ballistic projectile. These equations are taken from NATO-STANAG 4355 [9]. As the given equations show, in order to evaluate the trajectory of a spin stabilized projectile the aerodynamic coefficients for weapon and projectile such as $C_{D,0}$, $C_{L,\alpha}$, C_{mag} , mass and inertial moment of projectile and some factors such as form factor *i*, drag factor and muzzle velocity of projectile should be known. These variables are fire control data and should be known for the projectile and weapon that is going to be considered. Fire control data are generally grouped as inner and outer variables.

Inner variables are:

- Projectile mass
- Projectile geometry
- Projectile muzzle velocity
- Projectile spin

Outer variables are:

- Gravity
- Meteorological Conditions

These variables affect the azimuth and elevation angles of the projectile. The variation in mass, muzzle velocity, tail/front wind, density of air and temperature

affects the elevation angle. The variations in lateral wind, yaw of repose, coriolis force affects the azimuth angle of projectile.

3.4.2 Monte Carlo Simulation

In order to determine the standard deviations of miss distance of projectiles both in azimuth and elevation, a Monte Carlo simulation is implemented in this work. The variations in ballistic dispersion of weapon and projectile, muzzle velocity and wind speed are taken to be the main sources of random errors. The random errors used, are given in Table 3-1 with their assumed values of standard deviations.

Table 3-1: Standard deviations of random errors

Error Source	Standard Deviation Value	Unit
Projectile and weapon ballistic dispersion	1	mrad
Muzzle Velocity variation	7	m/s
Wind Speed	2	m/s

It is assumed that there is no target position error and aiming error. That is, there is no bias between the predicted hit point and actual target position. The only errors taken into consideration are dispersion type errors.

By implementing a Monte Carlo simulation, a large number of independent trials aimed at the diagonal center of the rectangular target area are used.

Simulation takes random inputs which are produced by random number generators in order to produce MPMM trajectory multiple times until normal distribution is achieved by the simulation. Number of iterations for the simulation is determined by a statistical test which is called “t-test”.

In order to determine the number of replications, a relative precision and confidence level should be determined. Simulation time depends on the values of these parameters. Since decreasing relative precision and increasing confidence level increase the simulation time.

In this work, the relative precision is taken to be 0.1 and 70% confidence interval of the miss distance in azimuth and elevation is determined. The interval is constructed such that the half-length of the interval around the mean value is less than or equal to 10% of the calculated mean and the mean value of miss distance is in the calculated confidence interval with a probability of 0.7. This value is the confidence interval of 1 σ standard deviation of a normal probability distribution. Normal probability density function is given in Section 3.2.

Random inputs resulting from different sources of errors are simulated with a normally distributed random number generator in MATLAB environment. The standard deviations (errors) are used to obtain instantaneous values of the inputs for MPMM model and azimuth and elevation miss distances for each instance is recorded. In order to test if the number of replications is enough to characterize a 70% confidence interval with 10% relative precision, t-test is used. If the precision of the confidence interval is not achieved at the end of replication number of simulation runs, a new replication number is proposed and simulation runs are taken up to the proposed replication number. The t-test procedure applied in this work and summarized above, works as follows [12]:

1. An initial number of replications n is determined. It is usually chosen to be a small number like 5, 10 or 20. In this work, this value is taken to be 20.
2. The results of performance variable are recorded n times which equals the initial number of replications (c_i 's for $1 \leq \mathrm{i} \leq \mathrm{n}$).
3. The mean of the performance variable is obtained according to Equation (3-19).

$$\bar{\bar{Y}} = \frac{\sum_1^n c_i}{n} \tag{3-19}$$

4. The standard deviation of the performance variable s, which is miss distance in this work, is obtained according to following equation.

$$s = \sqrt{\frac{\sum_1^n \left(c_i - \bar{\bar{Y}}\right)^2}{n-1}} \tag{3-20}$$

5. h is determined according to following equation where α is significance level.

$$h = t_{(n-1),\left(1-\frac{\alpha}{2}\right)} \frac{s}{\sqrt{n}} \tag{3-21}$$

A desired half length h^* is calculated using Equation (3-22) with given desired relative precision r taken to be 0.1.

$$h^* = r\,\bar{\bar{Y}} \tag{3-22}$$

6. If $h \leq h^*$ then simulation stops within confidence interval. ($\bar{\bar{Y}} \mp h$)
7. Otherwise,
   a. $n^* = \left[n\left(\frac{h}{h^*}\right)^2\right] + 1$ is calculated. Additional $(n^* - n)$ replications are done.

b. Then, n^* is taken to be equal to n and the algorithm is repeated to obtain the results satisfying the determined r and α with the determined initial number of replications.

Nominal trajectory is the trajectory of the projectile in standard conditions with zero error. It is needed to obtain miss distances caused from random errors. Thus, miss distance is taken to be the difference between the nominal trajectory and the erroneous trajectory. Nominal trajectory is simulated and the position of projectile at 1000 m, 2000 m, and 3000 m ranges are recorded. In order to obtain the nominal position of projectile at different ranges the basic inputs to MPMM trajectory are given in Table 3-2.

Table 3-2: Input values to MPMM

Inputs	**Value**
Mass of projectile	1.5 kg
Muzzle velocity of projectile	1000 m/s
Azimuth orientation angle	0°
Elevation orientation angle	45°
Speed of wind	5 m/s
Direction of wind	30°

Weapon orientation angles are taken with respect to weapon reference coordinate system. On the other hand, direction of wind is taken with respect to earth reference coordinate system. The schematic view of the firing of projectile with given values in Table 3-2, is illustrated in Figure 3.4.

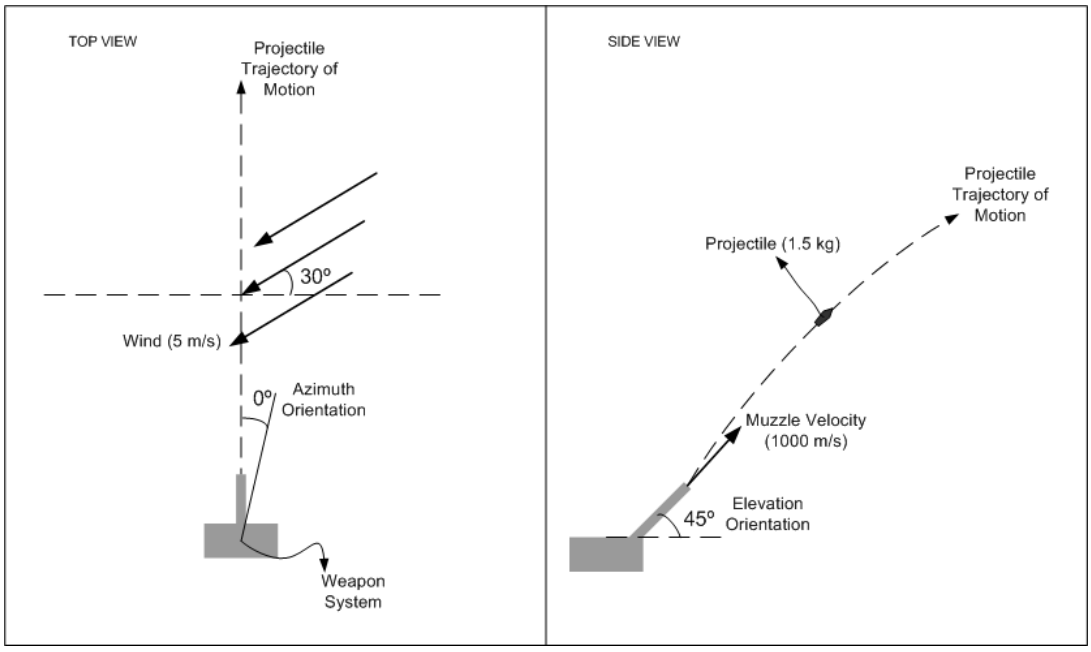

Figure 3.4: Schematic top and side views of projectile firing

The nominal position of projectile at different ranges is given in Table 3-3, with its azimuth and elevation positions.

Table 3-3: Nominal azimuth and elevation distances

Range (m)	**Azimuth Position (m)**	**Elevation Position (m)**
1000	0.20	705
2000	0.78	1404
3000	1.80	2098

The random inputs that are taken to obtain the standard deviations are produced by random number generator. Random number produced for weapon and projectile ballistic dispersion is added to azimuth orientation and elevation orientation angles of weapon pointing. Actually, the dispersion value in azimuth is added to azimuth orientation angle and dispersion value in elevation is added to elevation orientation angle. The random number produced for muzzle velocity variation is directly added

to muzzle velocity input of MPMM trajectory model. The random number produced for wind speed is added to wind vector which is again the input of MPMM trajectory model.

Numbers of iterations, standard deviations in azimuth and elevation directions are given, respectively, in Table 3-4 which is determined for ranges of 1000 m, 2000 m, and 3000 m.

Table 3-4: Azimuth and elevation standard deviations of miss distance

Range (m)	Number of Iterations	Azimuth Standard Deviation (m)	Elevation Standard Deviation (m)
1000	2786	0.70	0.82
2000	5377	1.43	1.52
3000	93335	2.14	2.24

From the determination of standard deviations, it can be concluded that with increasing range, error propagation increases and the standard deviations in azimuth and elevation increase. Moreover, number of replications increases with increasing range.

Ballistic dispersion of weapon and projectile are taken to be equal in both azimuth and elevation then, they have equal contributions to the miss distances in both directions. Muzzle velocity mostly contributes in elevation. Because azimuth of weapon orientation angle is 0°, there is no azimuth component of muzzle velocity at the firing instance. On the other hand, wind speed variation contributes to both the azimuth and elevation miss distances. In fact, the lateral wind component contributes to azimuth, but front wind component contributes to elevation miss distance.

In this work, however, analysis of each random error causing azimuth and elevation miss distances is out of the scope. The effects of different sources of errors can be determined with an error budget analysis. Moreover, the derived standard deviations of miss distance of projectile in azimuth and elevation directions at different ranges

are assumed to be the standard deviations of burst point of the projectile. These values of standard deviations are going to be used to analyze the different measures of effectiveness of airburst projectiles such as target coverage, number of sub-projectile hits on the target. Moreover, for Single Shot Kill Probability (SSKP) computation these values are going to be utilized. The details of SSKP computation and the results obtained are given in Chapter 4.

CHAPTER 4

METHODOLOGY

For effectiveness evaluation of airburst projectiles in this work, Single Shot Kill Probability (SSKP) is computed for two airburst projectiles which differ according to their sub-projectile distribution patterns, namely circular and ring shaped patterns. SSKP is computed at different ranges and for different burst distances. Three effectiveness measures for an airburst projectile to be effective against a target are:

- Target coverage
- Number of sub-projectiles hits on the target
- Kinetic energy of sub-projectiles

From these measures three lethality functions are determined. These functions are utilized to compute SSKP for airburst projectiles. Computation results are used to compare the effectiveness and to determine the optimum burst distances of two different distribution patterns.

4.1 Expected Coverage Area Computation

Airburst projectiles eject their sub-projectiles in front of the target and generally sub-projectiles are enclosed in a circular area. When burst point is assumed to be at the center of the pattern, coverage area for an airburst projectile turns out to be a rectangular and circular intersection area computation.

With the inclusion of the randomness of the burst point with respect to predicted hit point, expected value of coverage area can be determined. The burst point is assumed to have a normal distribution both in azimuth and elevation directions and they are

assumed to be independent. Moreover, it is assumed that there is no bias error, that is, the mean values of the distribution are taken to be zero. (Figure 4.1)

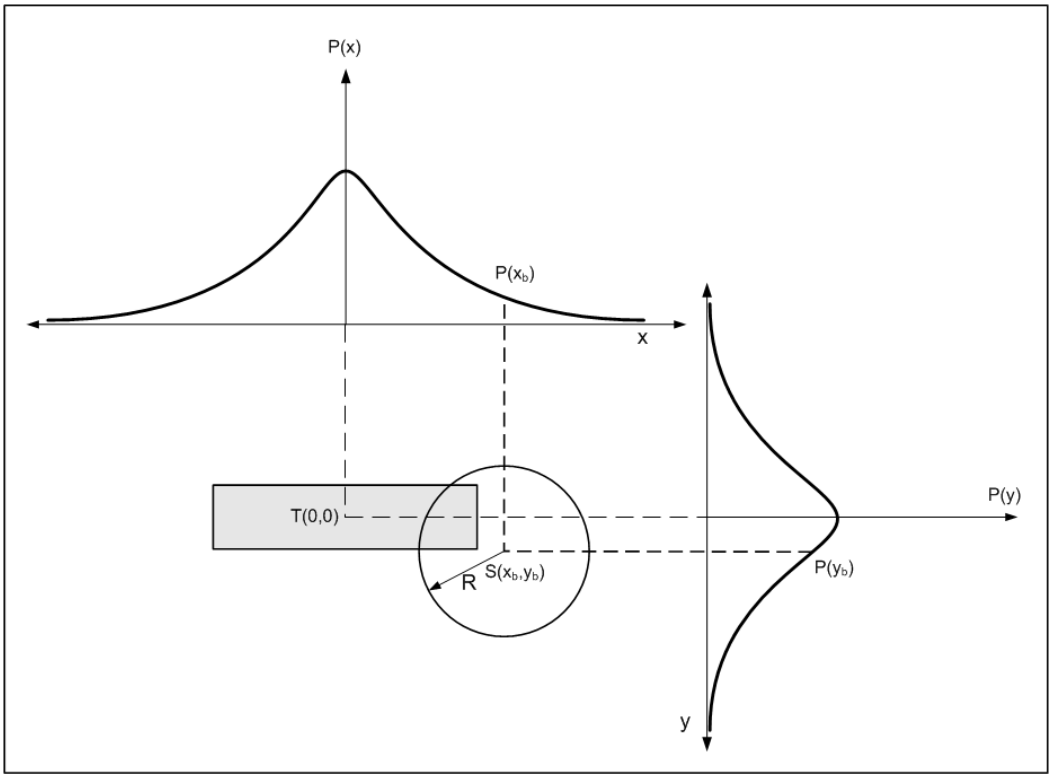

Figure 4.1: Bivariate normal distribution of burst points

Then expected coverage area E_A can be computed by using Equation (4-1).

$$\mathrm{E_A} = \frac{1}{2\pi\sigma_x\sigma_y}\int_{-\infty}^{\infty}\int_{-\infty}^{\infty}\mathrm{A_c(x,y)e}^{-\frac{1}{2}\left(\frac{x_b^2}{\sigma_x^2}+\frac{y_b^2}{\sigma_y^2}\right)}\mathrm{dxdy} \qquad (4\text{-}1)$$

where:

$A_c(x, y)$: The coverage area

$(x_b\ , y_b)$: Position of burst point

σ_x: Standard deviation in x-direction

σ_y: Standard deviation in y-direction

Finding the coverage area $A_c(x, y)$ of rectangular target and sub-projectile circular pattern is mainly a circle-rectangle cross-section area calculation problem shown by Figure 4.2.

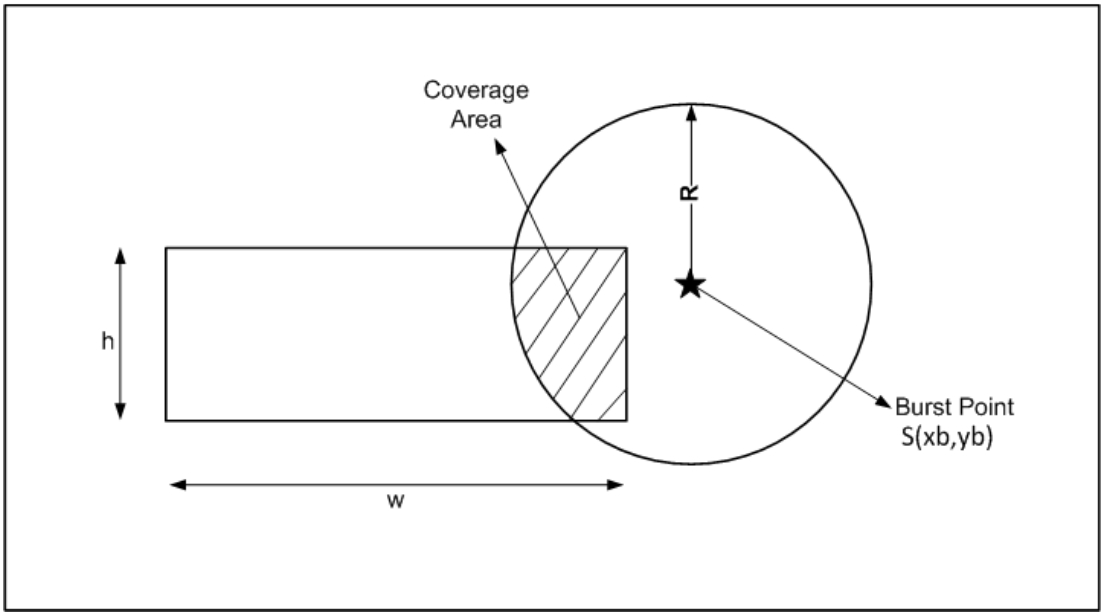

Figure 4.2: Coverage area representation

Coverage area can be analytically computed by separating the problem into conditions (many different conditions such as "rectangle is fully inside the circle" or "circle is fully inside the rectangle" can be defined). However, this is a long procedure to apply. Instead, it is possible to calculate intersection area numerically by defining infinitesimal elements which are Δx, Δy in x and y directions, respectively.

$$A_c(x,y) \sim \sum_{i=-w/2}^{w/2} \sum_{j=-h/2}^{h/2} a\left(x_i, y_j\right) \Delta x \Delta y \qquad (4\text{-}2)$$

where:

w: Width of the rectangular area

h: Height of the rectangular area

(x_i, y_j): Position of the infinitesimal element of the rectangular area

$a\left(x_i, y_j\right)$: Given by Equation (4-4)

In this work, in order to compute the intersection area Δx, Δy are taken to be equal to 0.01. For example, with this value rectangular area, with dimensions of 2.5 m in width and 0.3 m in height, is divided in to 250 to 30 infinitesimal area elements. $a\left(x_i, y_j\right)$ is a function defined to be 1, 0, or ½ according to the condition if the infinitesimal area element is inside, outside or on the border of the circle. At the border condition the value is assumed to be ½. Decreasing the infinitesimal area element dimensions increases the simulation time.

In order to define $a\left(x_i, y_j\right)$ a function $D(x,y)$ giving the distance between a point (x,y) and the center a circle (x_b, y_b) having radius R is used. This function is utilized to check the position of the area elements with respect to border of circular area (Figure 4.3).

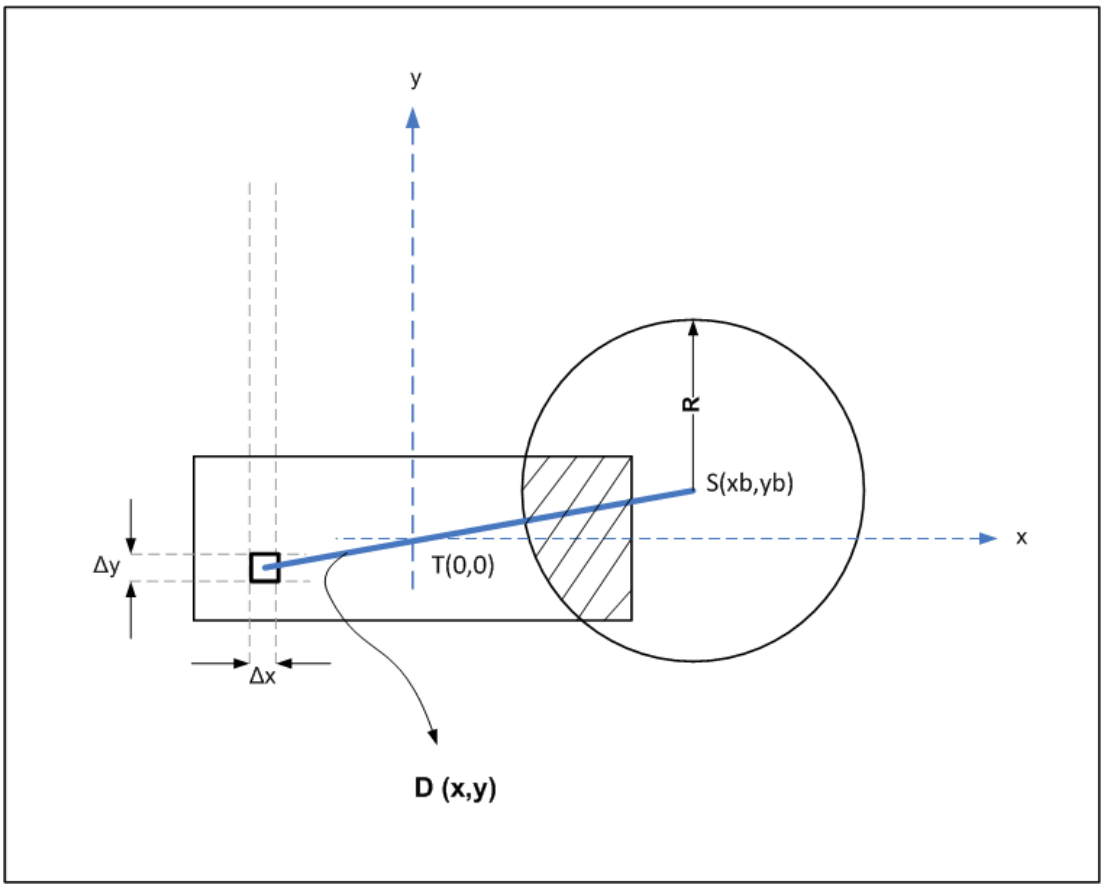

Figure 4.3: Coverage area computation

The expression related to the function $D(x, y)$ is given in Equation (4-3).

$$\mathrm{D(x,y)} = \sqrt{(\mathrm{x_b} - \mathrm{x})^2 + (\mathrm{y_b} - \mathrm{y})^2} \tag{4-3}$$

Then;

$$\mathrm{a}(\mathrm{x_i}, \mathrm{y_j}) = \begin{cases} 0, & \text{if} \quad \mathrm{D}(\mathrm{x_i}, \mathrm{y_j}) > R \\ \frac{1}{2}, & \text{if} \quad \mathrm{D}(\mathrm{x_i}, \mathrm{y_j}) = \mathrm{R} \\ 1, & \text{if} \quad \mathrm{D}(\mathrm{x_i}, \mathrm{y_j}) < R \end{cases} \tag{4-4}$$

where

R: Radius of the circular pattern

(x_i, y_j): Position of the area element of rectangular area

In order to compute the coverage area of a different pattern, namely ring shaped pattern, same procedure is applied. In order to compute coverage area equations (4-1) and (4-2) directly applies to this case. Moreover, the expression related to the function $D(x, y)$ is taken to be the same which is expressed with Equation (4-3). Only the function $a(x_i, y_j)$ is changed to the function $a_r(x_i, y_j)$, which has the expression given by Equation (4-8).

$$a_r\left(x_i, y_j\right) = \begin{cases} 0, & \text{if} \quad \left(D\left(x_i, y_j\right) > r_1\right) \;||\; \left(D\left(x_i, y_j\right) < r_2\right) \\ \frac{1}{2}, & \text{if} \quad \left(D\left(x_i, y_j\right) = r_1\right) \;||\; \left(D\left(x_i, y_j\right) = r_2\right) \\ 1, & \text{if} \quad r_2 < D\left(x_i, y_j\right) < r_1 \end{cases} \tag{4-5}$$

where

(x_i, y_j): Position of the area element of rectangular area

r_1 : Outer radius of ring pattern

r_2 : Inner radius of ring pattern

4.2 Expected Number of Sub-projectile Hits Computation

Another criterion for effectiveness consideration of airburst projectile is the number of sub-projectile hits on the target. Since airburst projectiles carry their destructive potential with the aid of sub-projectiles, increasing the number of sub-projectile hits on the target, will result in a higher damage.

Sub-projectiles are assumed to be uniformly distributed in the area of propagation for different patterns in this work. The number of sub-projectile hits on the target, which

is again an expected value designated as E_N, can be determined. The expression for this measure is given by Equation (4-6).

$$E_N = N \frac{E_A}{A_s} \tag{4-6}$$

where

N : Number of sub-projectiles inside a projectile

A_s: Sub-projectiles area of propagation

4.3 Analysis of Different Measures of Effectiveness

In this section, different measures of effectiveness are going to be analyzed for airburst projectiles. These measures are target coverage, number of sub-projectile hits on the target, and kinetic energy of sub-projectiles after burst. Actually, target coverage and number of sub-projectile hits on the target are expected values but the kinetic energy of a sub-projectile is determined from Modified Point Mass Model (MPMM) which is a deterministic value.

In order to see the effect of a different sub-projectile distribution on target coverage, number of sub-projectile hits on the target and optimum burst distance, a different distribution pattern is also analyzed. The pattern is a ring shaped pattern. The main difference of this pattern from circular pattern is it has a smaller area of propagation, that is, it propagates towards target with a high density of sub-projectiles with the same number of sub-projectiles N in its body.

In order to analyze different measures of effectiveness in this work, a representative missile target dimension is used. Missile dimension is approximated with a rectangular area which has a width of 2.5 m and height of 0.3 m [7]. Moreover, target

area is assumed to be of equal importance. That is to say, no weight is assigned for different parts of the target area.

The predicted hit point is assumed to be the center of rectangular target area. The determined standard deviations of miss distances in azimuth and elevation directions explained in Section 3.4.2 are assumed to be the standard deviations of the burst point of airburst projectile. Moreover, it is assumed that there is no dispersion of projectile in longitudinal direction.

During the analyses burst angle of airburst projectile is assumed to be 10°. Moreover, this angle is taken to be constant for different ranges. In this work, the radius of sub-projectile coverage (R) increases with increasing burst distance (d). The relation between burst distance and burst angle is illustrated by Figure 4.4.

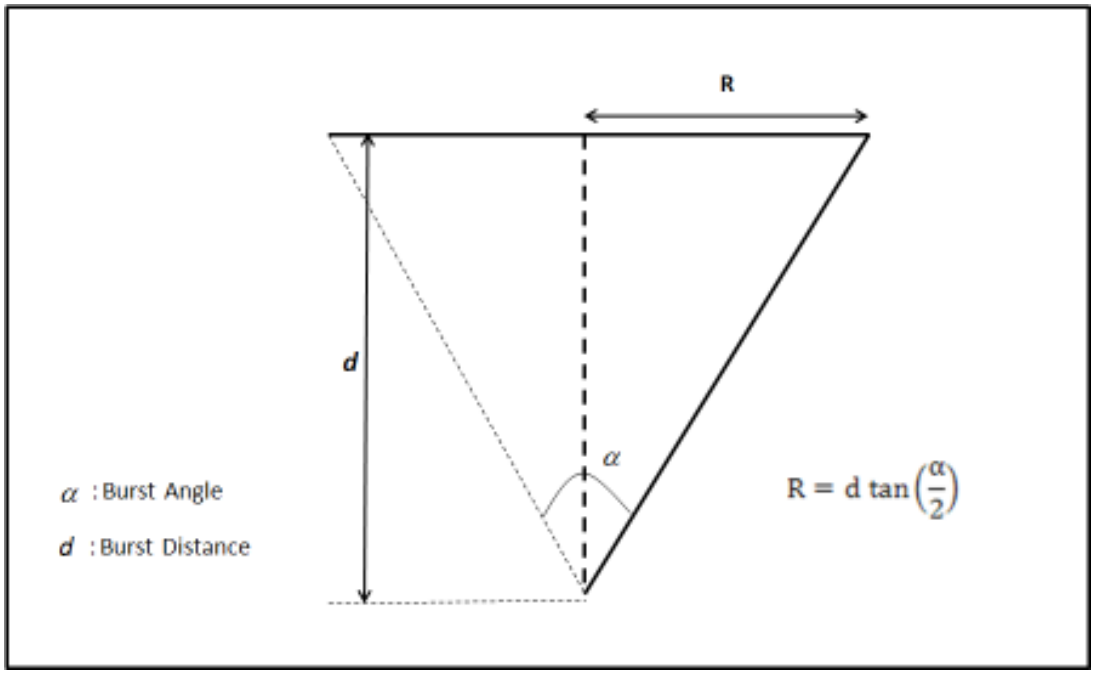

Figure 4.4: Relation between burst angle and burst distance

4.3.1 Target Coverage

For airburst projectiles, increasing burst distance increases target coverage but decreases the number of sub-projectile hits on the target, and vice versa. Therefore, there is an effective value of burst distance that should have to be determined for an effective airburst projectile. Target coverage is an important measure of effectiveness for airburst projectiles in the sense of being effective against targets. Target coverage is the expected coverage area E_A of the target.

Target coverage is determined according to Equation (4-1) with the determined standard deviations given in Section 3.4.2 resulting from different sources of random errors at different ranges. The result of target coverage with respect to increasing burst distance for circular pattern is shown in Figure 4.5. Target coverage is normalized with the target area, which is equal to 0.75 m^2, for the illustrations in this work.

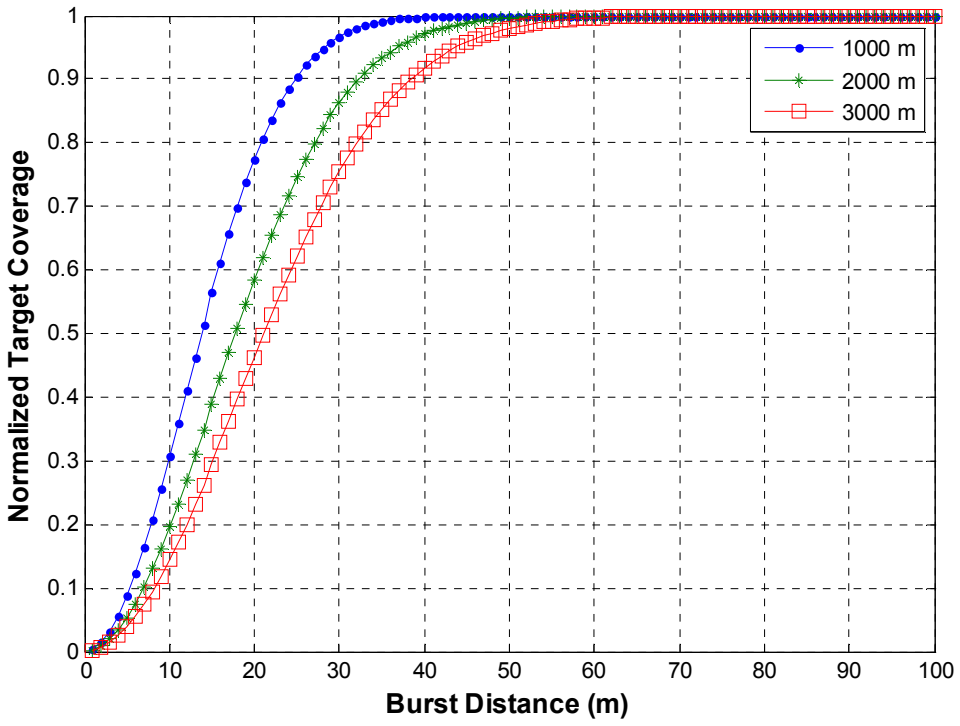

Figure 4.5: Target coverage for circular pattern

For different ranges, target coverage increases with increasing burst distance. At the same range, target is partially covered up to a specific burst distance. Increasing burst distance above this value result in full target coverage at all ranges.

In order to see the effect of different $\frac{r_2}{r_1}$ ratios, different ring patterns are analyzed in terms of target coverage. At a range 1000 m, the results of target coverage for different ring patterns are shown in Figure 4.6.

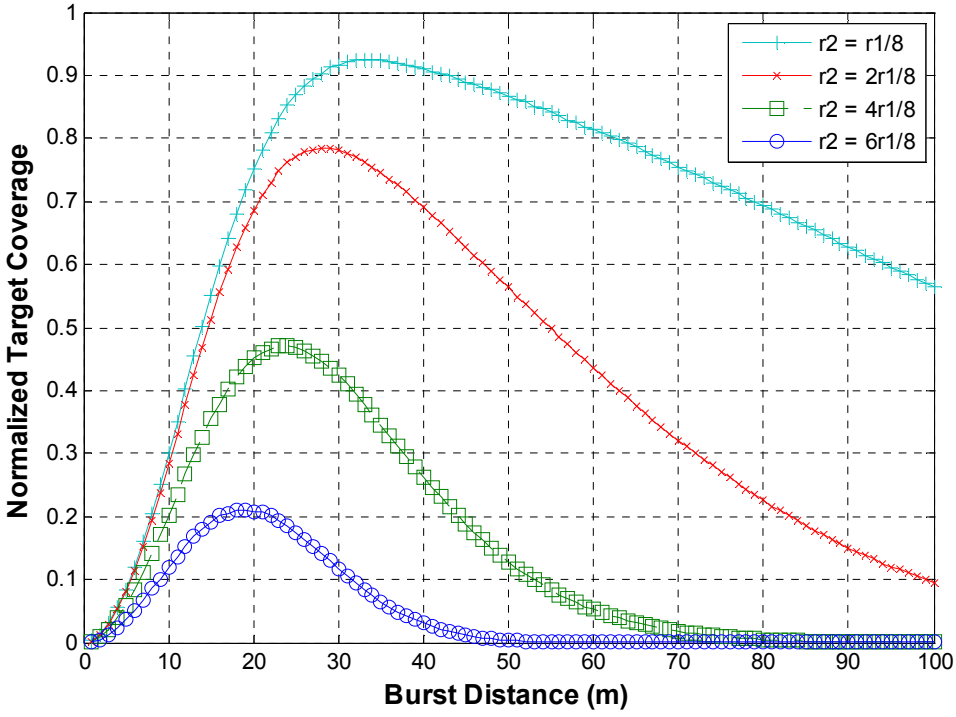

Figure 4.6: Target coverage for different r_2/ r_1 ratios for ring pattern

For ring pattern with decreasing $\frac{r_2}{r_1}$ ratio the result approaches to the result of target coverage for circular pattern.

In order to see the effect of different ranges on target coverage for ring pattern a ratio of ½ is chosen. The result of target coverage with respect to increasing burst distance for ring pattern is shown in Figure 4.7. Results are normalized with target area.

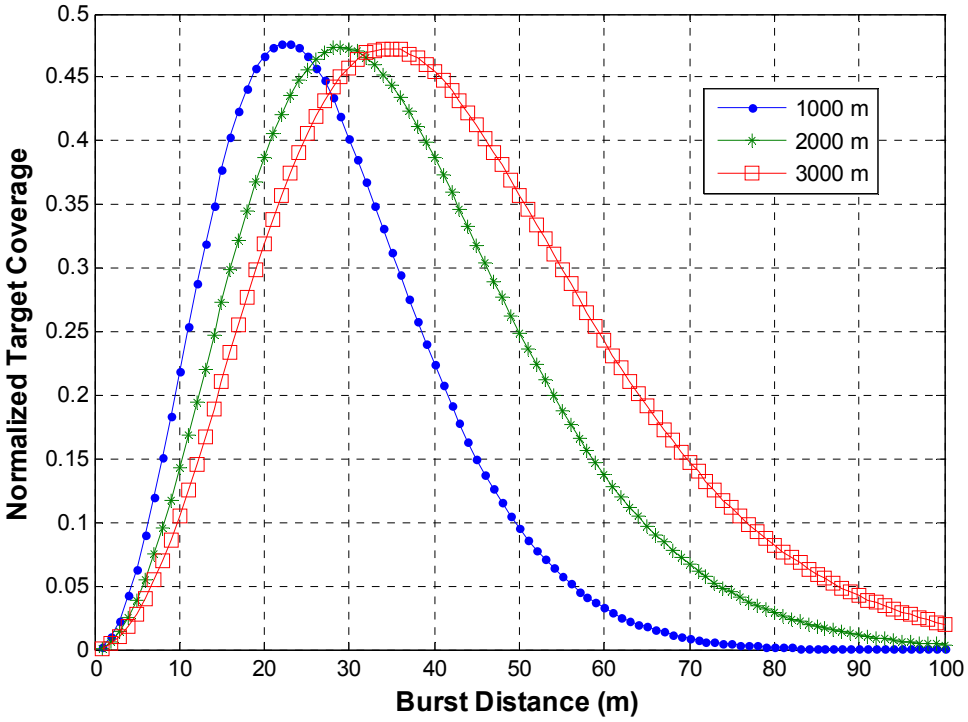

Figure 4.7: Target coverage for ring pattern with r_2/ r_1 ratio of ½

When the results at different ranges are compared; for small burst distances target coverage is high for low ranges but high for high ranges. The result shows that ring pattern is different from circular pattern in terms of target coverage. For different ranges, target is always partially covered for ring pattern. Target coverage has a maximum value at a specific burst distance. Increasing burst distance above this value decreases target coverage. Optimum burst distances and target coverage values at different ranges are given in Table 4-1.

According to the results obtained for the target coverage of ring pattern, the maximum target coverage achieved at different ranges is the same which is 0.47.

Table 4-1: Burst distances of maximum target coverage

Range (m)	Burst Distance (m)	Target Coverage
1000	23	0.47
2000	29	0.47
3000	35	0.47

4.3.2 Number of Sub-projectile Hits

With the determined standard deviations given in Section 3.4.2 resulting from different sources of random errors at different ranges, E_N with respect to increasing burst distance for circular pattern is shown Figure 4.8. E_N is normalized with the number of sub-projectiles (N) inside a projectile, for the illustrations in present study.

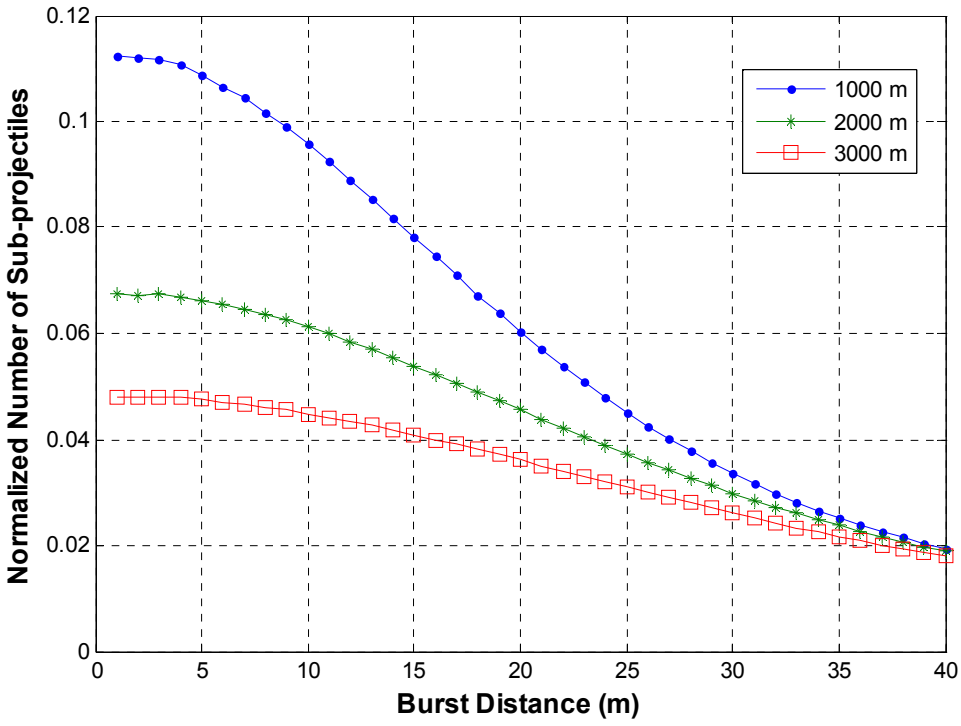

Figure 4.8: Number of sub-projectile hits for circular pattern

At the same range, number of sub-projectiles decreases with increasing burst distance. The highest number of sub-projectiles is achieved at the very small burst distances. When the results of all ranges are compared; number of sub-projectiles is low for high ranges. This is due to increasing standard deviations of random errors with increasing range.

In order to see the effect of different $\frac{r_2}{r_1}$ ratios, different ring patterns are analyzed in terms of number of sub-projectile hits measure. At a range 1000 m, the results of number of sub-projectile hits for different ring patterns are shown in Figure 4.9.

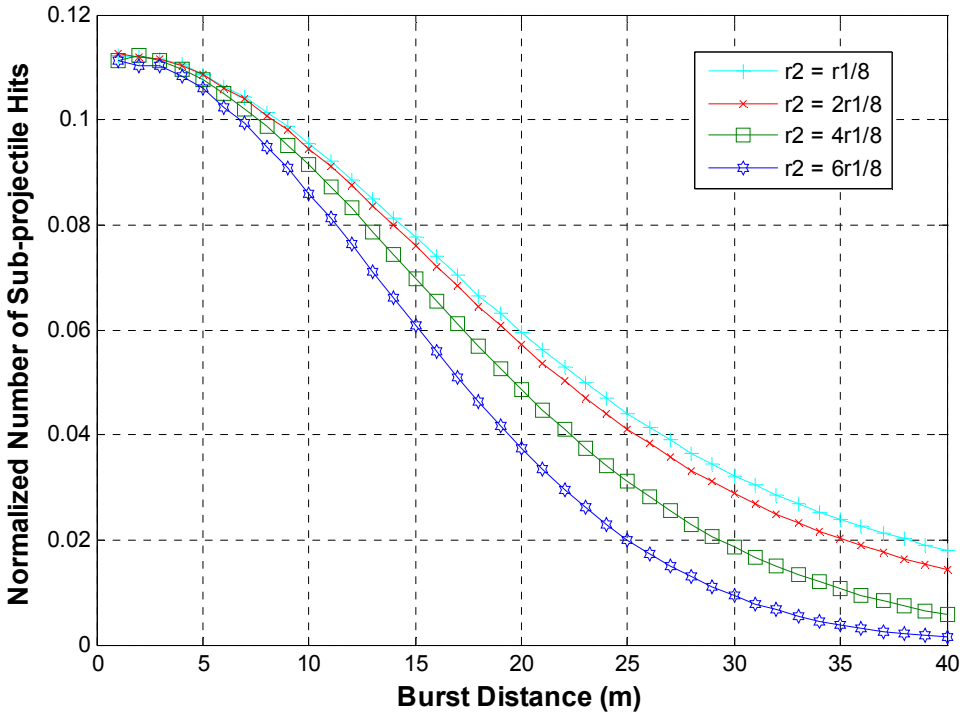

Figure 4.9: Number of sub-projectile hits for different r_2/ r_1 ratios for ring pattern

For all different $\frac{r_2}{r_1}$ ratios, number of sub-projectile hits decreases with respect to increasing burst distances. In order to see the effect of different ranges on number of sub-projectile hits for ring pattern a ratio of ½ is chosen. For this chosen ratio number of sub-projectiles that hit the target with respect to increasing burst distance

for ring pattern is shown in Figure 4.10. The number of sub-projectiles is normalized with total number of sub-projectiles N of the projectile.

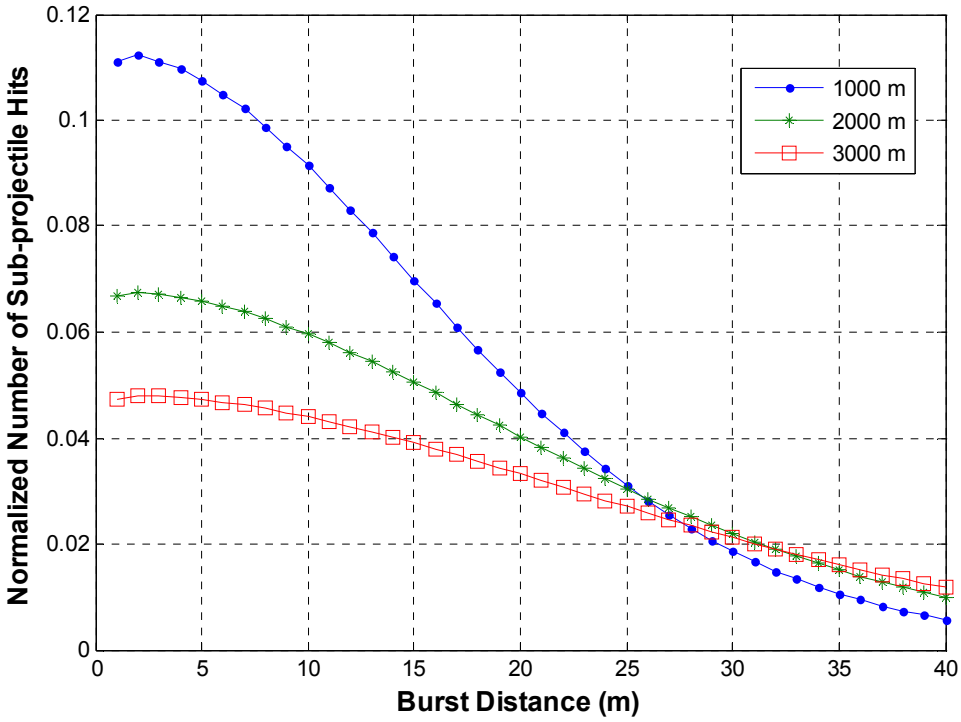

Figure 4.10: Number of sub-projectile hits for ring pattern with r_2/ r_1 ratio of ½

Number of sub-projectile hits decreases at all ranges with respect to increasing burst distance. This is the same result obtained for circular pattern. As expected, the highest number of sub-projectiles is achieved at the very small burst distances. Actually, the density of sub-projectiles is high at small burst distances and it decreases with increasing burst distance since the area of sub-projectile coverage increases.

4.3.3 Maximum Effectiveness

According to the results obtained for circular pattern, in order to maximize the projectile effectiveness, that is to adjust burst distance that will result in a maximum projectile effectiveness two effectiveness measures which are target coverage and number of sub-projectile hits are utilized. Maximum projectile effectiveness M_{eff} is the expected value of the squared coverage area (Equation (4-7)). This is because coverage area is the common term for both target coverage and number of sub-projectile hits.

$$M_{eff} = \frac{1}{2\pi\sigma_x\sigma_y}\int_{-\infty}^{\infty}\int_{-\infty}^{\infty} A_c(x,y)^2 e^{-\frac{1}{2}\left(\frac{x_b^2}{\sigma_x^2}+\frac{y_b^2}{\sigma_y^2}\right)} dxdy \qquad (4\text{-}7)$$

Normalized value of the result with respect to increasing burst distance at different ranges is given by Figure 4.11. The normalization is done with the multiplication of target area (A_T), sub-projectiles area of propagation (A_s), and number of sub-projectiles (N) inside a projectile. In fact, M_{eff} is divided by the result of this multiplication.

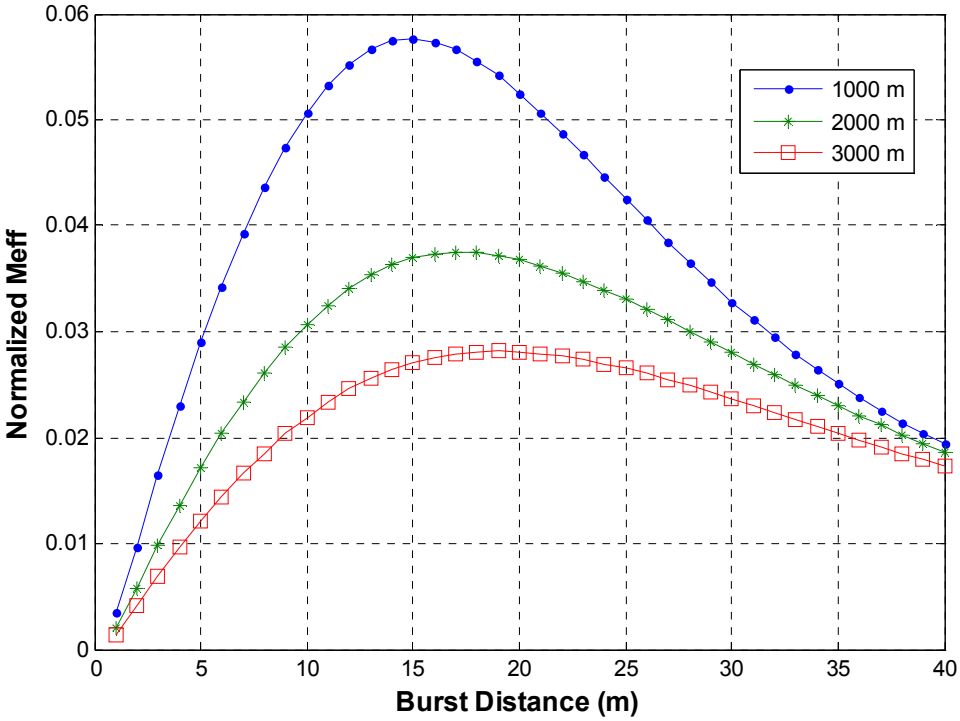

Figure 4.11: Maximum effectiveness for circular pattern

M_{eff}, at all three different ranges, has peak values. Burst distances giving this maximum values can be determined to be the optimum burst distances of airburst projectiles with circular pattern. The optimum burst distances, target coverage and sub-projectiles, respectively, are given by Table 4-2 for different ranges.

Table 4-2: Results for circular pattern

Range (m)	Burst Distance (m)	Target Coverage	Number of Sub-projectile Hits
1000	15	0.56	0.078
2000	17	0.47	0.051
3000	19	0.43	0.037

When range increases, it is evident that target coverage and number of sub-projectiles decrease. The maximum achievable target coverage is 0.56; number of sub-projectile hits is 0.078. Since these results are normalized, 0.56 target coverage refers to a coverage area of 0.42 m^2. Besides, a projectile having 100 sub-projectiles, hit target with approximately 8 sub-projectiles, at a range of 1000 m.

For ring pattern, in order to maximize the projectile effectiveness the same procedure is applied as for circular pattern.

In order to see the effect of different $\frac{r_2}{r_1}$ ratios, different ring patterns are analyzed in terms of maximum effectiveness. Normalized M_{eff} with respect to increasing burst distance at different ranges is given in Figure 4.12 at a range of 1000 m. M_{eff} is normalized with the multiplication of target area A_T, sub-projectiles area of propagation A_s, and number of sub-projectiles (N) inside a projectile.

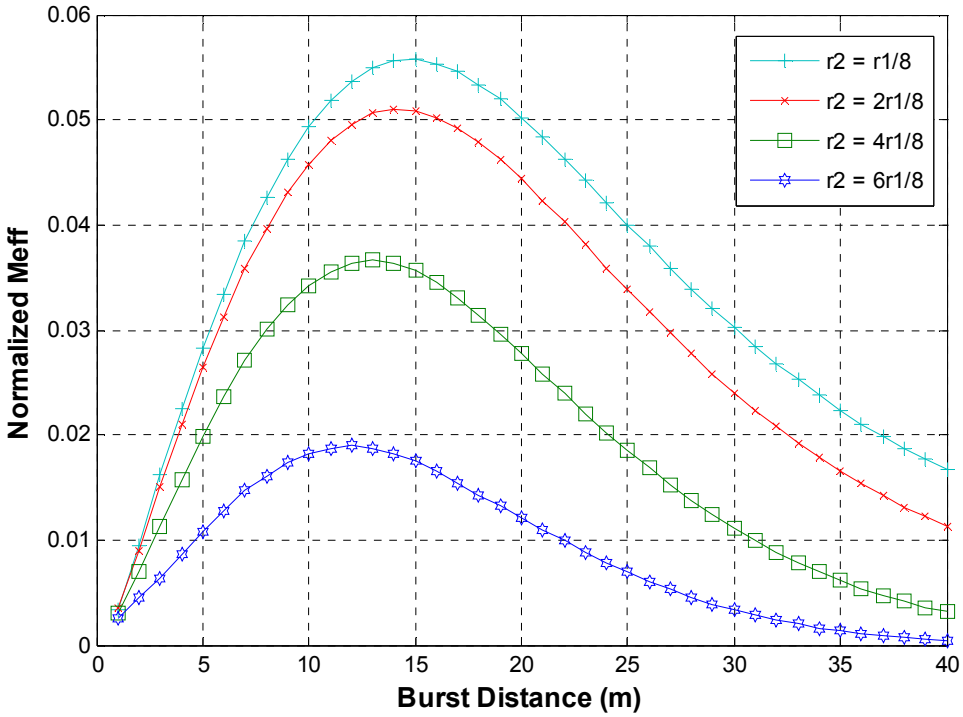

Figure 4.12: Maximum effectiveness for different r_2/ r_1 ratios for ring pattern

For all different $\frac{r_2}{r_1}$ ratios M_{eff} with respect to increasing burst distances have peak values. The burst distance satisfying these peak values are given in Table 4-3. According to the results obtained optimum burst distances increase with decreasing ratio of $\frac{r_2}{r_1}$.

Table 4-3: Optimum burst distances for different r_2/ r_1 ratios for ring pattern

Type of Ring Pattern	**Burst Distance (m)**
$^3/_4$ ratio	12
$^1/_2$ ratio	13
$^1/_4$ ratio	14
$^1/_8$ ratio	15

In order to see the effect of different ranges on maximum effectiveness for ring pattern a ratio of ½ is chosen. Maximum effectiveness M_{eff} with respect to increasing burst distance for ring pattern is shown in Figure 4.10. The number of sub-projectiles is normalized with total number of sub-projectiles (N) of the projectile.

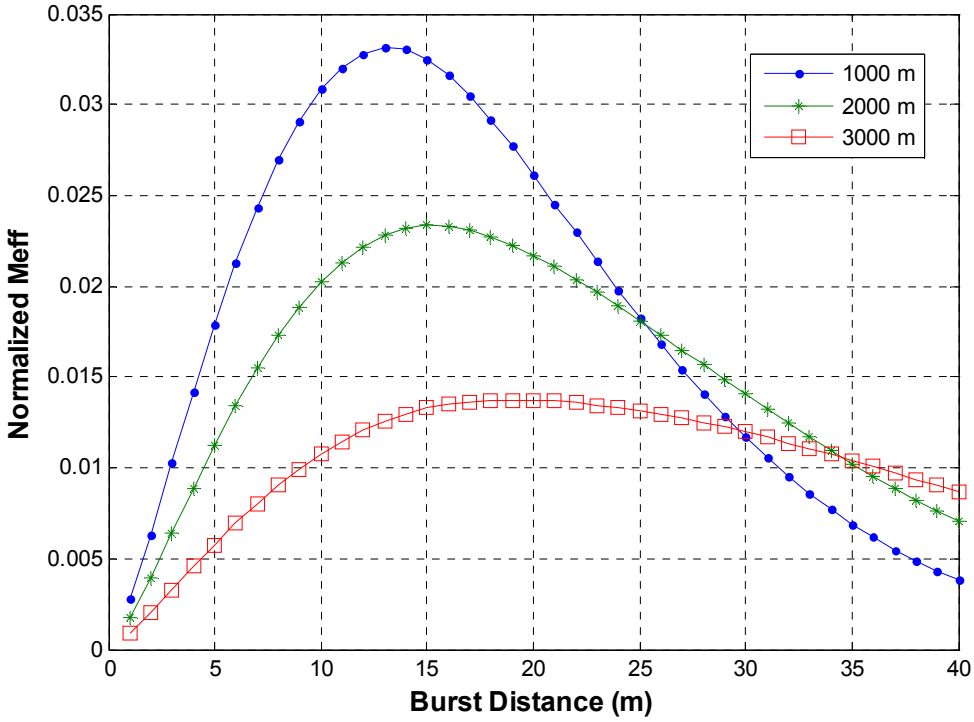

Figure 4.13: Maximum effectiveness for ring pattern with r_2/ r_1 ratio of ½

M_{eff}, at all three different ranges, has peak values. Burst distances giving this maximum values can be determined to be the optimum burst distances of airburst projectiles with ring pattern. The optimum burst distances, target coverage and number of sub-projectiles, respectively, are given in Table 4-4 for different ranges.

Table 4-4: Results for ring pattern

Range (m)	**Burst Distance (m)**	**Target Coverage**	**Number of Sub-projectile Hits**
1000	13	0.32	0.079
2000	15	0.27	0.051
3000	17	0.26	0.037

When range increases it is evident that target coverage and number of sub-projectiles decrease. The maximum achievable target coverage is 0.32, number of sub-projectiles is 0.079. The results of target coverage are less than the results of circular pattern but, number of sub-projectile hits is nearly the same for both patterns.

4.3.4 Kinetic Energy of Sub-projectiles

After the two measures of effectiveness are analyzed the third measure which is the kinetic energy of sub-projectiles is going to be determined. The kinetic energy of sub-projectiles mainly depends on two distances. One is the weapon to burst point distance and other is burst point and target distance. Kinetic energy of a projectile decreases with increasing weapon to burst point distance. Similarly, the kinetic energy of sub-projectiles decrease with increasing burst point to target distance, that is, burst distance *d*.

Modified Point Mass Model trajectory equations are used in order to determine speed of projectile with a mass of 1.5 kg at different ranges. The speed of the projectile is given in Table 4-5.

Table 4-5: Nominal speeds for projectile

Range (m)	Speed of Projectile (m/s)
1000	975
2000	951
3000	929

At different ranges, it is assumed that the speed of a single sub-projectile is the same of projectile at the time of burst and mass of a single projectile is taken to be 1.5 g, and then each sub-projectile has a kinetic energy as given in Table 4-6.

Table 4-6: Kinetic energy of a sub-projectile

Range (m)	Kinetic Energy (Joule)
1000	713
2000	678
3000	647

It is assumed that there is no velocity decrement due to burst point to target distance, that is, sub-projectiles propagate towards target with constant speed.

4.4 Single Shot Hit Probability Computation

Single shot hit probability P_H given by Equation (3-4) is valid for projectiles that do not burst in the air. However, for airburst projectile this equation is not valid since airburst projectiles affect larger areas on the target as shown in Figure 4.14.

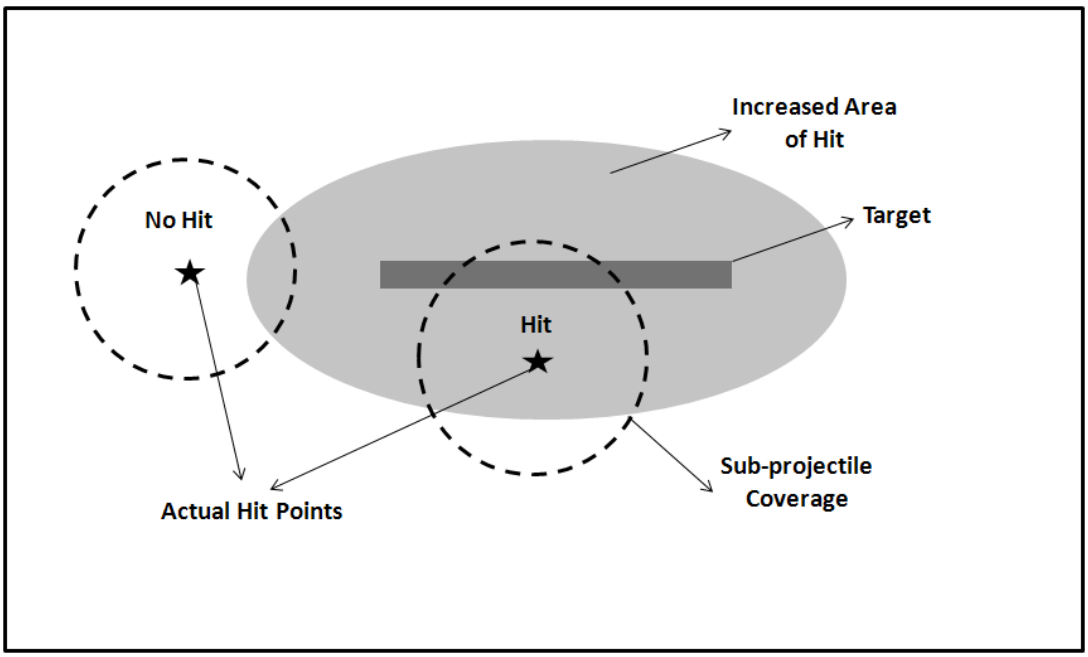

Figure 4.14 : Hit and no hit condition for airburst projectiles

In order to compute P_H for two different types of airburst projectiles a plenty of assumptions are made. These are:

1. The predicted hit point is assumed to be the center of the target.
2. In order to represent error, bivariate normal probability density function is used. It is assumed that the variants are independent and there is no mean of errors. The standard deviations determined in Section 3.4 are going to be used in the computation of SSHP.
3. The hit criteria is going to be such that if any subprojectile hits the target area it is going to be evaluated as a hit. (Figure 4.14)
4. No hit criteria is going to be such that if no subprojectile hits the target area it is going to be evaluated as a no hit. (Figure 4.14)
5. Target is going to be a rectangular area with width of 2.5 m and height of 0.3 m.

For circular pattern P_H with respect to increasing burst distance is shown in Figure 4.15.

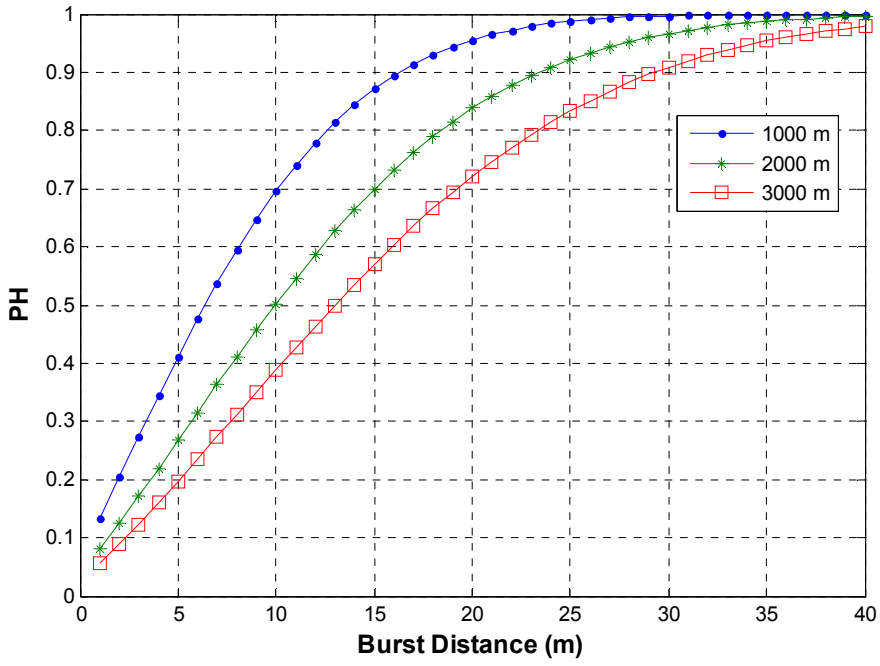

Figure 4.15: P_H vs. burst distance for circular pattern

For ring pattern, P_H computation is considered for a pattern with a $\frac{r_2}{r_1}$ ratio of ½. For this specific case, P_H with respect to increasing burst distance is shown in Figure 4.16.

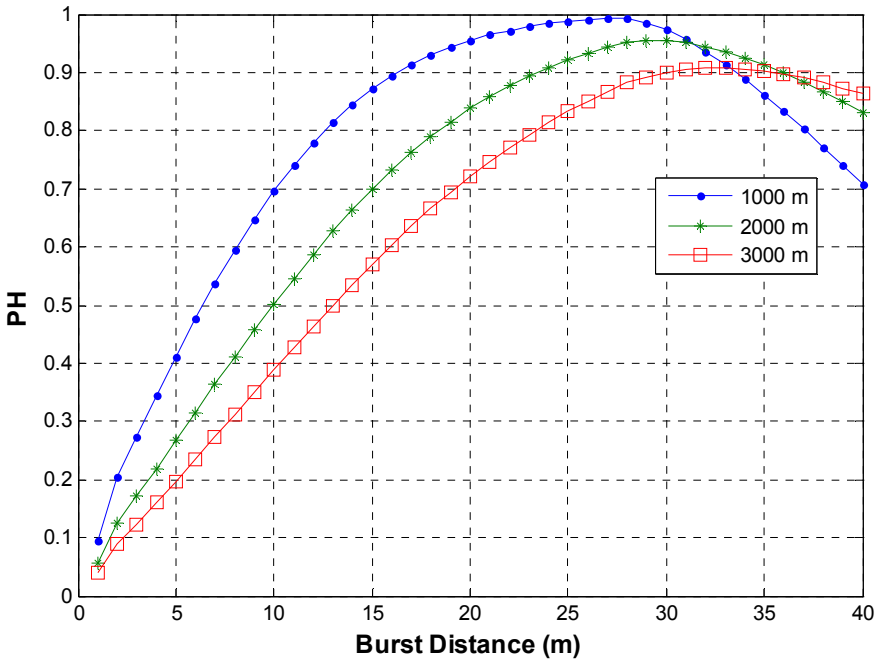

Figure 4.16: P_H vs. burst distance for ring pattern with r_2/ r_1 ratio of ½

According to SSHP compuation results maximum achievable SSHP values differ for each different sub-projectile distribution pattern. For circular pattern, at high burst distances it is possible to obtain an SSHP value of 1. For ring pattern, however, it is not possible to obtain a value of 1. For this pattern the highest values are obtained at different burst distances. Burst distances satisfying maximum SSHP at different ranges are given in Table 4-7.

Table 4-7: Peak P_H values and burst distances for ring pattern

Range (m)	P_H	Burst distance (m)
1000	1.00	28
2000	0.95	30
3000	0.90	34

On the other hand, it can be concluded that SSHP only represents the target coverage measure for airburst projectiles. Therefore, in this work, in order to evaluate effectiveness for airburst projectiles, a comprehensive way is carried out. This is Single Shot Kill Probability (SSKP).

4.5 Single Shot Kill Probability Computation

For an airburst projectile, in order to satisfy a specific level of damage, target coverage, number of sub-projectile hits on the target, and the kinetic energy of sub-projectiles should be taken into account. In order to determine lethality function P_L three lethality functions are generated.

Lethality functions related to target coverage and kinetic energy of sub-projectile are defined with sigmoid functions. However, the lethality function which is related with the number of sub-projectile hits on the target is defined as a linear function of E_N, the expression of which is given by Equation (4-6).

For determination of the lethality function with respect to target coverage, a ratio C_r is defined. The expression of C_r is given by Equation (4-8).

$$C_r = \frac{E_A}{A_T} \tag{4-8}$$

where

E_A: Target coverage

A_T: Target area

Lethality function P_{L1} is defined as a sigmoid function that is equal to 1 for $C_r \geq 0.8$ and is equal to 0 for $C_r \leq 0.2$. These upper and lower values of C_r are taken from available documents. Between these values lethality due to target coverage changes obeying an s-shaped curve which is sigmoid function. Sigmoid function is an s-shaped curve, the equation of which is given by Equation (4-8) and it is suitable for the determination of lethality functions.

$$f(x) = \frac{1}{1 + e^{\frac{-(x-\alpha)}{\beta}}} \tag{4-9}$$

This function maps $[-\infty, +\infty]$ interval into$[0,1]$. α and β determine the center and width of the function, respectively. The variation of P_{L1} with respect to coverage ratio C_r is given in Figure 4.17.

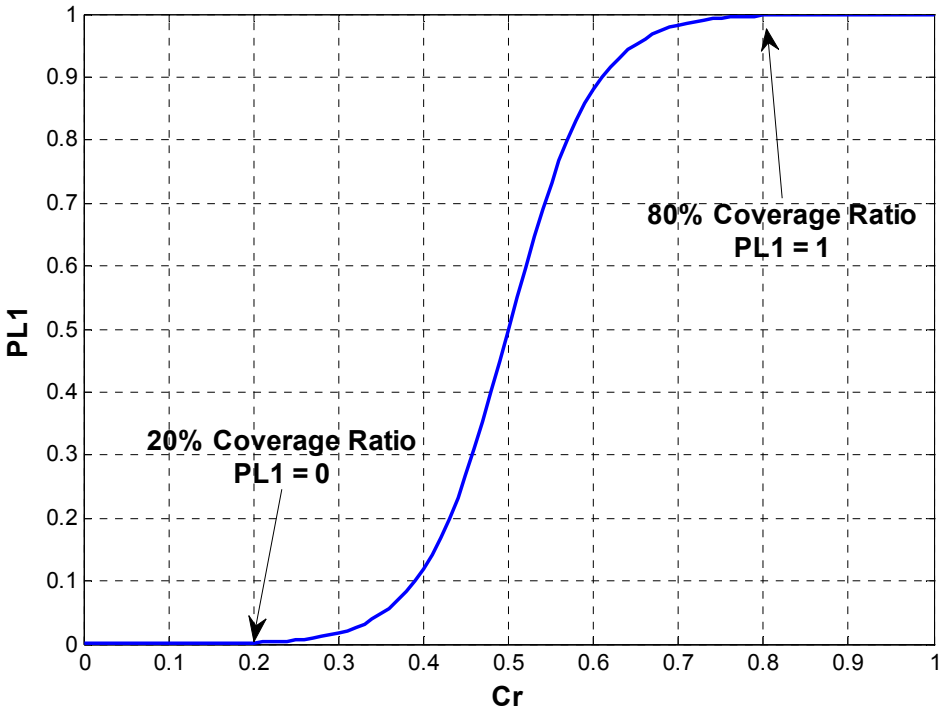

Figure 4.17: Lethality due to target coverage

Next, the lethality function which is related with the number of sub-projectile hits on the target, P_{L2} is defined. It is a linear function of expected number of sub-projectile hits on the target E_N (Equation (4-10)).

$$P_{L2} = \frac{E_N}{N} \tag{4-10}$$

The variation of P_{L2} with respect to E_N is shown in Figure 4.18. N, the number of sub-projectiles inside a projectile, is taken to be 181 for this lethality consideration [1].

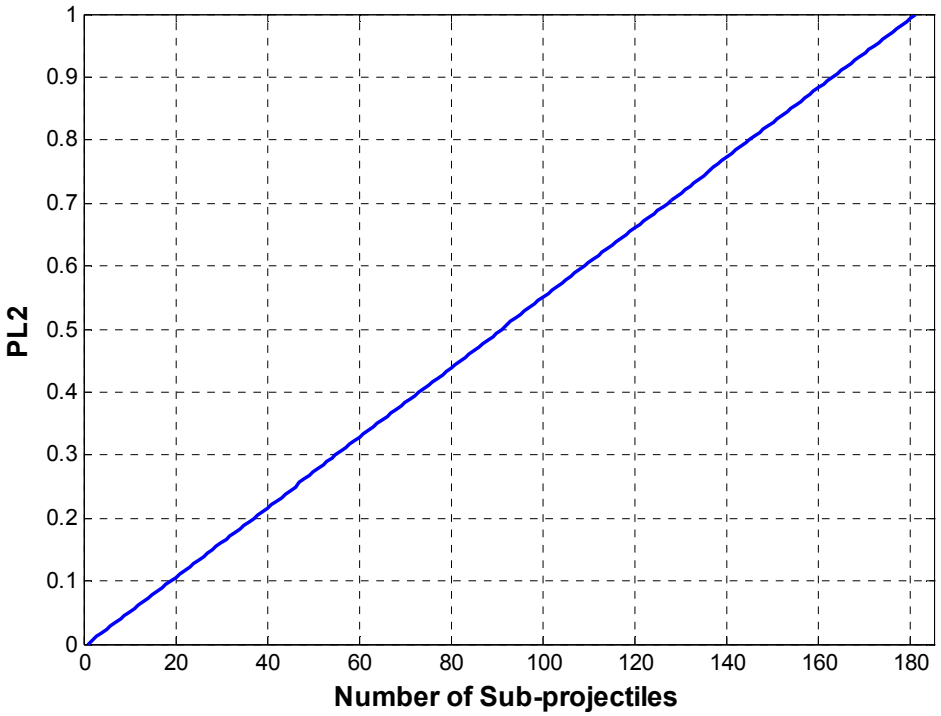

Figure 4.18: Lethality due to number of sub-projectiles

In order to determine the lethality function with respect to kinetic energy of a single sub-projectile, the lethality function P_{L3} is defined as a sigmoid function that is equal to 1 for $KE_{sp} \geq 900$ J and is equal to 0 for $KE_{sp} \leq 300$J. These upper and lower values of KE_{sp} are also taken from available documents same as C_r. Between these values lethality due to kinetic energy of a sub-projectile changes obeying the sigmoid function. The variation of P_{L3} with respect to KE_{sp} is given in Figure 4.19.

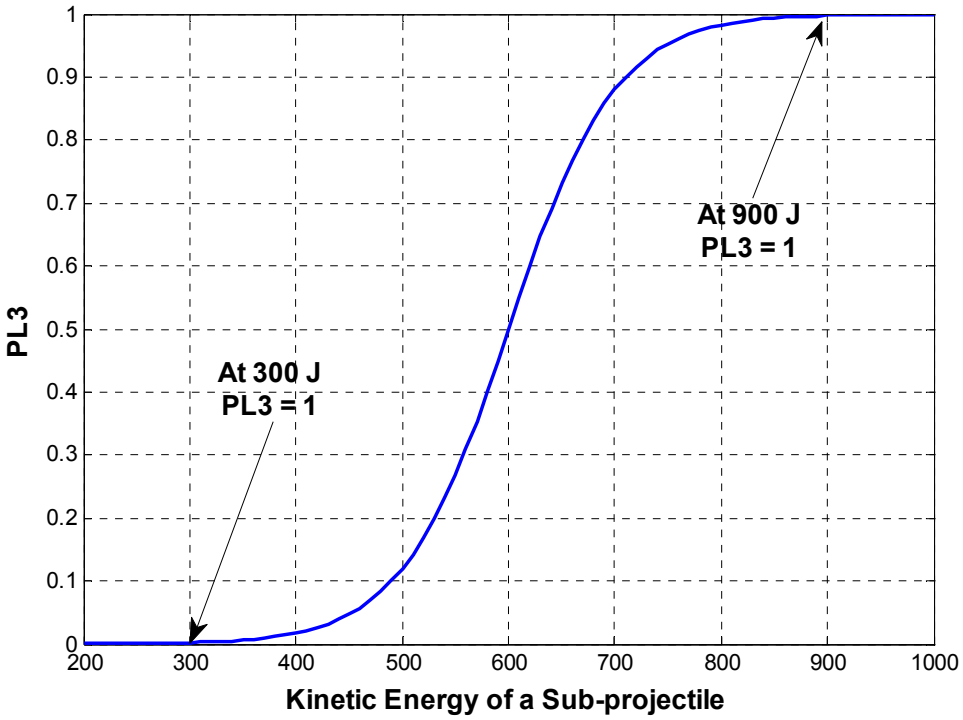

Figure 4.19: Lethality due to kinetic energy of a sub-projectile

With the generated lethality functions the overall lethality P_L can be computed. Lethality functions are assumed to be independent of each other. Then, the expression of P_L is given by Equation (4-11).

$$P_L = P_{L1} \text{ x } P_{L2} \text{ x } P_{L3} \tag{4-11}$$

Then the SSKP is computed by the multiplication of P_L and P_H. The expression of SSKP P_K is given by Equation (4-12)

$$P_K = P_L \text{ x } P_H = P_{L1} \text{ x } P_{L2} \text{ x } P_{L3} \text{ x } P_H \quad (4\text{-}12)$$

Considering the generated lethality functions and standard deviations of burst point of airburst projectile in azimuth and elevation, Single Shot Kill Probability (SSKP) is computed for airburst projectiles. In this work, the variation of SSKP with respect to increasing burst distance is analyzed. This is applied to two different types of airburst projectile according to their distribution patterns which are circular and ring shaped patterns. A plenty of assumptions are made during the SSKP computations. These are as follows:

1. Different distribution patterns of sub-projectiles are assumed to be symmetric with respect to the longitudinal axis of projectile. Different patterns are characterized with uniformly distributed sub-projectile densities.
2. All sub-projectiles of a projectile are assumed to impact on the target plane at the same time with the same velocities.
3. Projectile's kinetic energy is transferred to sub-projectiles with no loss of energy. Moreover, it is assumed that there is no velocity decrement for sub-projectiles due to air drag in the travelling distance of burst point to target.
4. The determined standard deviations of miss distance in azimuth and elevation directions in Section 3.4.2 are used in SSKP computation. They are taken to be the standard deviations of burst point of airburst projectiles.
5. There is no dispersion of burst point in the longitudinal axis of motion of the projectile. This is because the target is taken to be a two dimensional rectangular area, and no penetration analysis is carried out in the scope of this thesis.

For circular pattern, Single Shot Kill Probability (SSKP) P_K with respect to increasing burst distance is given in Figure 4.20. The results are obtained for different ranges.

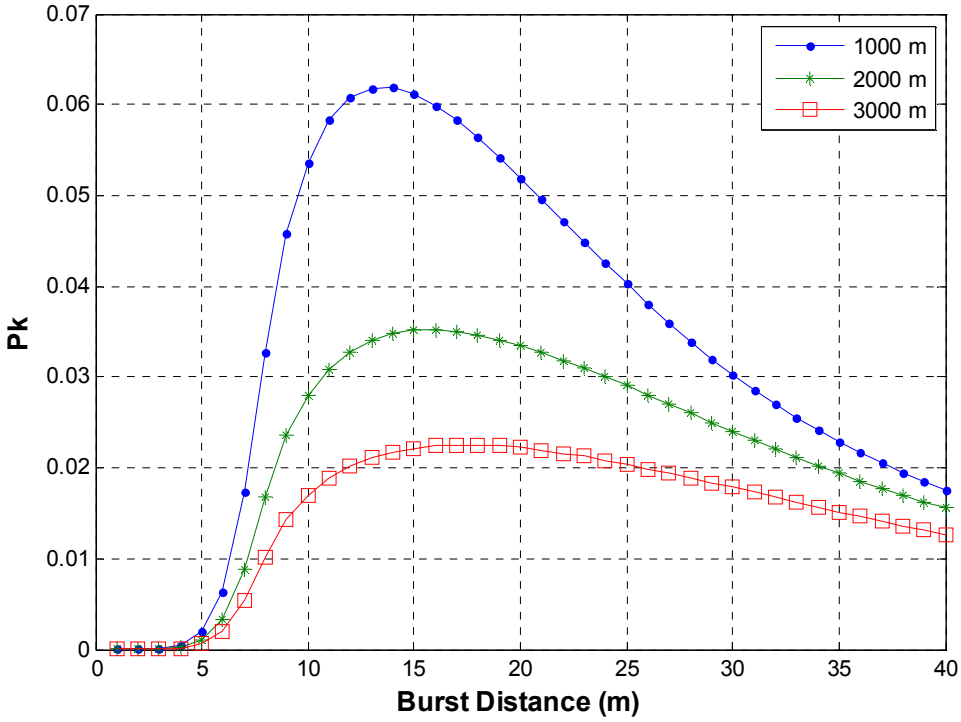

Figure 4.20: P_K vs. burst distance for circular pattern

According to peak values of P_K at different ranges, optimum burst distances are given in Table 4-8.

Table 4-8: Peak P_K values and optimum burst distances for circular pattern

Range (m)	P_K	**Burst distance (m)**
1000	0.062	14
2000	0.035	16
3000	0.023	17

As the range increases, P_K decreases and the optimum burst distance increases. According to the results it can be concluded that for a single airburst projectile P_K is very small. In fact, a single airburst projectile cannot be effective against a missile

target with this value of P_K. On the other hand, with increasing range, optimum burst distances slightly increase.

In order to see the effect of different pattern in SSKP computations, a ring pattern with $\frac{r_2}{r_1}$ ratio of ½ is chosen. For this pattern, P_K with respect to increasing burst distance is given in Figure 4.21.

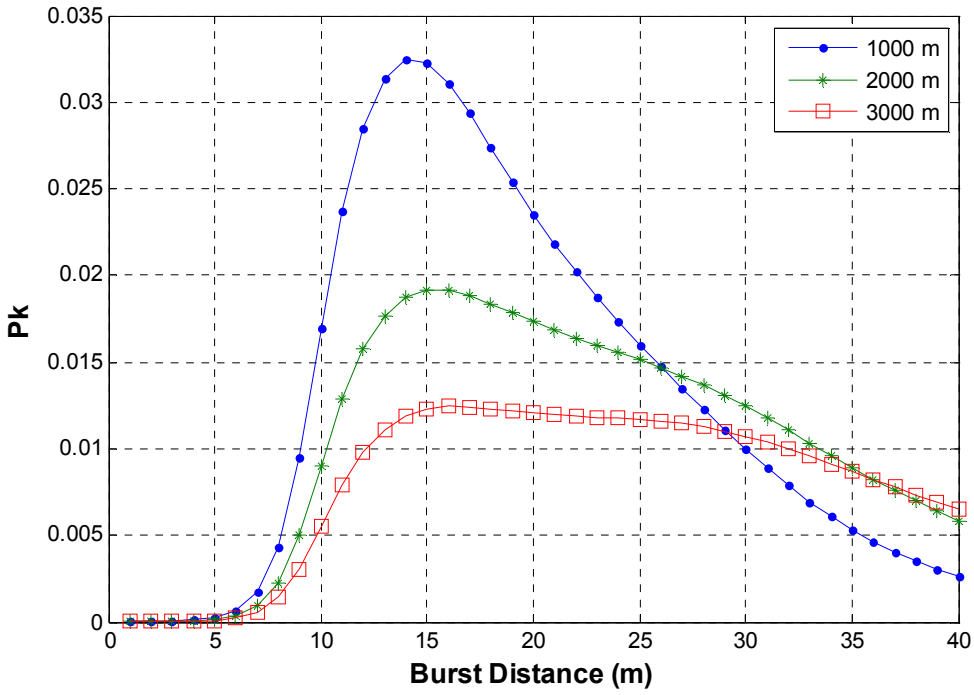

Figure 4.21: P_K vs. burst distance for ring pattern

According to peak values of P_K for different ranges, optimum burst distances are given in Table 4-9.

Table 4-9: Peak P_K values and optimum burst distances for ring pattern

Range (m)	P_K	Burst distance (m)
1000	0.032	14
2000	0.019	15
3000	0.012	16

Comparing with circular pattern, for ring pattern at different ranges, P_K decreases but it is nearly the half of the values obtained for circular pattern. Then it can be concluded that an airburst projectile with ring pattern is less effective than an airburst projectile with circular pattern according to the assumptions made during this work and the results of P_K values. On the other hand, for ring pattern the optimum burst distance increases with increasing range.

According to the results of optimum burst distances determined from SSKP computation results for ring pattern optimum burst distances are slightly smaller than circular pattern.

When results of optimum burst distances for both patterns are compared with the results of study [1]; they are small in this work. This is because in that study a larger target was used. Target was ellipsoid shaped with dimensions of 5 m to 10 m. However, in this work, a rectangular target with width of 2.5 m and height of 0.3 m is utilized. Different from the results of that study, increasing range increases burst distance in this study. Because when range increases, the deviation of projectile's burst point increases. In order to satisfy equal area coverage at increasing ranges burst distance should be increased. But the effect of uncertainties is the same for two studies, that is, with increasing uncertainty burst distance increases.

According to the results of SSKP computation, it can be suggested that airburst projectile with circular pattern be used as they have higher SSKP values. Moreover, instead of using this projectile to defeat a target at high ranges, it is suggested to utilize this projectile at low ranges such as 1000 m.

CHAPTER 5

CONCLUSION

In this work, for effectiveness evaluation of airburst projectiles, three measures are determined. These are target coverage, number of sub-projectile hits on the target and kinetic energy of sub-projectiles after burst. Two different sub-projectile distribution patterns are analyzed in terms of different measures of effectiveness. Then, single shot hit and kill probabilities are computed for these projectiles. Single Shot Kill Probability (SSKP) is computed at different burst distances. Three lethality functions are used to compute SSKP. These lethality functions are determined from different measures of effectiveness which are target coverage, number of sub-projectile hits and kinetic energy of sub-projectiles. Different sub-projectile distribution patterns of airburst projectiles utilized are circular and ring patterns. The results obtained at different ranges, are used to compare the effectiveness of two different types of airburst projectiles and to determine optimum burst distances of each projectile.

For circular pattern, with increasing burst distances, target coverage increases and number of sub-projectiles decreases. On the other hand, increasing range results in less target coverage and number of sub-projectile hits on the target. For ring pattern with increasing burst distances target coverage increases up to a specific value and then starts decreasing. However, number of sub-projectile hits always decreases as burst distance increases.

According to the results of Single Shot Hit Probability (SSHP) for different types of airburst projectiles, it is possible to obtain high probability values. However, maximum hit probabilities are achieved at high burst distances when compared with the optimum burst distances determined from Single Shot Kill Probability (SSKP) computation for maximum kill probabilities. According to the results of SSKP

computation, two projectiles are different in terms of effectiveness. For ring pattern there is constant SSKP values in a range of burst distances at high ranges. In fact, in that range, increasing or decreasing burst distance does not change the kill probability values for ring pattern. Moreover, a projectile with circular pattern is more effective than a projectile with ring pattern based on the assumptions and the procedure applied in this work.

In hit and kill probability computation a ring pattern with a $\frac{r_2}{r_1}$ ratio of ½ is used. Increasing this ratio results in higher hit and kill probability values, decreasing this ratio results in lower hit and kill probability values. In fact, increasing this ratio causes the pattern to approach circular pattern.

Computation of SSKP depends on lethality functions. Therefore, determining lethality functions is crucial to evaluate the effectiveness of airburst projectiles. The upper and lower values of lethality functions are taken from available documents. However, in real world, these lethality functions should be determined according to target to be defeated and the aim of air defense.

In this work, target vulnerability characteristics are not considered. All parts of the target are assumed to be of equal importance. However, this is not true for the real world. There are always some parts of target which are critical to achieve its mission. Therefore, as a future work, with the inclusion of vulnerability characteristics of target, effectiveness of airburst projectiles can be reanalyzed.

REFERENCES

[1] Türkuzan, Mehmet. "Increasing Air Defense Capability by Optimizing Burst Distance" Ankara : Middle East Technical University, 2010. M.Sc. Thesis.

[2] Boss, Andre. "Method and Device for Determining the Disaggregation Time of a Programmable Projectile" 5814756 Switzerland, 29 September 1998.

[3] Kloten, Peter Toth. "Method For Increasing The Probability of Air Defense By Means of A Remotely Fragmentable Projectile" 5322016 Switzerland, 21 Jun 1994.

[4] Washburn, Alan. "Diffuse Gaussian Multiple-Shot Pattern" s.l. : *Military Operations Research*, 2003. Vol.8, No.3.

[5] Handbook, Department of Defense. Fire Control Systems-General. s.l. : Department of Defense, 1996. MIL-HNDK-799 (AR).

[6] Pfeilsticker, Robert C. Dziwak, Walter J. "Design Methodology For Satisfying Fleet Weapon Performance Requirements" New Jersey : *U.S. Army Armament Research, Development and Engineering Center,* 1998. ARFSD-TR-98003.

[7] Wachsberger, C. Lucas, M. Krstic, A. "Limitations of Guns as a Defence against Manoeuvring Air Weapons" Edinburgh : *Australian Government Department of Defence Systems Sciences Laboratory*, 2004. AR-013-117.

[8] Fann, Chee Meng. "Development of An Artillery Accuracy Model" Monterey : Naval Postgraduate School, 2006.

[9] NATO. NATO Standardization Aggrement (STANAG) "The Modified Point Mass and Five Degrees of Freedom Trajectory Models" 2005. STANAG 4355.

[10] [Online] Arrow Tech Associates. [Last Accessed Date: 25 May 2011.] http://www.prodas.com/tutorials/yawcd/ycrd_190.htm.

[11] Nash, David A. "Modeling the In-Flight and Terminal Properties of Ballistic Munitions" Monterey : s.n., 1992.

[12] Kelton, W. David. Sadowski, Randall P. Sturrock, David T. "Simulation with Arena" 2003.

[13] Anderson, Colin Michael. "Generalized Weapon Effectiveness Modeling" Monterey : Naval Postgraduate School, 2004. Thesis.